NASA Technical Memorandum 100023

Flap-Lag Equations of Motion of Rigid, Articulated Rotor Blades with Three Hinge Sequences

Robert T. N. Chen, Ames Research Center, Moffett Field, California

November 1987

National Aeronautics and
Space Administration

Ames Research Center
Moffett Field, California 94035

TABLE OF CONTENTS

NOMENCLATURE

A_1	symbol used to represent a gravitational term, $A_1 = \sin i \cos \phi_a \cos \theta_a - \cos i \sin \theta_a$
A_2	symbol used to represent a gravitational term, $A_2 = \sin \phi_a \cos \theta_a$
A_3	symbol used to represent a gravitational term, $A_3 = \cos i \cos \phi_a \cos \theta_a + \sin i \sin \theta_a$
A_{1s}	lateral cyclic pitch measured from hub plane and in hub-body system, rad (or deg)
a_x, a_y, a_z	components of total linear acceleration at the aircraft center of gravity expressed in the hub-body system, ft/sec^2 (m/sec^2)
B	tip loss factor
B_{1s}	longitudinal cyclic pitch measured from hub plane and in hub-body system, rad (or deg)
c	blade chord, ft (m)
c_d	blade section drag coefficient
c_ℓ	blade section lift coefficient
C_β	flapping damper coefficient, lb-ft-sec/rad (N-m-sec/rad)
C_ζ	lag damper coefficient, lb-ft-sec/rad (N-m-sec/rad)
c.g.	center of gravity
dD	incremental drag force on blade element, lb (N)
dL	incremental lift force on blade element, lb (N)
e_β	flapping hinge offset, ft (m)
e_ζ	lag hinge offset, ft (m)
Δe	distance between the flapping and lag hinges, ft (m)
g	gravitational acceleration, ft/sec^2 (m/sec^2)
i	tilt angle of the rotor shaft in the rotorcraft x_a-z_a plane, positive tilt forward, rad (deg)

I_ζ	mass moment of inertia of the rotor blade about the lag hinge, slug-ft^2 (kg-m^2)
I_β	mass moment of inertia of the rotor blade about the flapping hinge, slug-ft^2 (kg-m^2)
$I_{\Delta e}$	mass moment of inertia of the rotor blade segment between the flapping and lag hinges about the inner hinge (flapping or lag hinge), slug-ft^2 (kg-m^2)
K_1	pitch-flap coupling ratio
K_2	pitch-lag coupling ratio
K_β	flapping spring constant, lb-ft/rad (N-m/rad)
K_ζ	lag spring constant, lb-ft/rad (N-m/rad)
ℓ_x, ℓ_y, ℓ_z	components of the offset between the aircraft center of gravity and the hub center in hub-body system (ℓ_x positive when the hub center is forward of aircraft c.g.; ℓ_y positive when the hub center is to the right of aircraft c.g.; ℓ_z positive when the hub center is below aircraft c.g.), ft (m)
m	mass of blade per unit of radius, slug/ft (kg/m)
m_ζ	mass of blade from lag hinge to blade tip, slug (kg)
m_β	mass of blade from flapping hinge to blade tip, slug (kg)
M_r	local Mach number at blade element (M_r = U/a, with a being the speed of sound)
M_ζ	mass moment of rotor blade about lag hinge in a horizontal position, slug-ft (kg-m)
M_β	mass moment of rotor blade about flapping hinge in a horizontal position, slug-ft (kg-m)
$M_{\Delta e}$	mass moment of rotor blade segment between the flapping and lag hinge about the inner hinge (flapping or lag hinge depending on a hinge sequence) in a horizontal position, slug-ft (kg-m)
p,q,r	components of aircraft angular velocity in hub-body system, rad/sec (or deg/sec)
$\dot{p},\dot{q},\dot{r}$	components of aircraft angular acceleration in hub-body system, rad/sec^2 (or deg/sec^2)

Q_{ζ_1} generalized force associated with lead-lag for L-F-P hinge sequence, lb-ft/rad (N-m/rad)

Q_{β_1} generalized force associated with flapping for L-F-P hinge sequence, lb-ft/rad (N-m/rad)

Q_{ζ_2} generalized force associated with lead-lag for F-P-L hinge sequence, lb-ft/rad (N-m/rad)

Q_{β_2} generalized force associated with flapping for F-P-L hinge sequence, lb-ft/rad (N-m/rad)

Q_{ζ_3} generalized force associated with lead-lag for F-L-P hinge sequence, lb-ft/rad (N-m/rad)

Q_{β_3} generalized force associated with flapping for F-L-P hinge sequence, lb-ft/rad (N-m/rad)

$Q_{\zeta,A}, Q_{\beta,A}$ aerodynamic force contribution to the generalized force associated with lead-lag and flapping, respectively (different expressions for the three hinge sequences), lb-ft/rad

$Q_{\zeta,G}, Q_{\beta,G}$ gravitational force contribution to the generalized force associated with lead-lag and flapping, respectively (different expressions for the three hinge sequences), lb-ft/rad

$Q_{\zeta,D}, Q_{\beta,D}$ contribution of dampers to the generalized force associated with lead-lag and flapping, respectively, lb-ft/rad

$Q_{\zeta,S}, Q_{\beta,S}$ contribution of hub springs to the generalized force associated with lead-lag and flapping, respectively, lb-ft/rad

r_ζ radial position of the blade element measured from the lag hinge, ft (m)

r_β radial position of the blade element measured from the flapping hinge, ft (m)

r_c radius of blade root pocket cutout (i.e., radius at which lifting surface of blade begins), ft (m)

R rotor blade radius measured from the center of rotation, ft (m)

T total kinetic energy of a blade, lb-ft (N-m)

U resultant relative air velocity perpendicular to blade-span axis at blade element, ft/sec (m/sec), $U = (u_T^2 + u_P^2)^{1/2}$

u_T	component at the blade element of resultant relative air velocity perpendicular to the blade-span axis and on the plane parallel to x_1-y_1 plane, ft/sec (m/sec)
u_P	component at blade element of resultant relative air velocity perpendicular to both the blade-span axis and u_T, ft/sec (m/sec)
u_S	component at blade element of resultant relative air velocity along the blade span, ft/sec (m/sec)
V_r	total inertial velocity of the blade element, ft/sec (m/sec)
δW_t	total virtual work done on the blade by an external force, lb-ft (N-m)
x,y,z	hub-body system
x',y',z'	inertia system
x_a,y_a,z_a	body-axis system
$\dot{x}_o,\dot{y}_o,\dot{z}_o$	components of velocity at the aircraft center of gravity in hub-body system, ft/sec (m/sec)
$\dot{x},\dot{y},\dot{z}$	components of velocity at blade element due to rotation, flapping, pitching, and lagging motion (i.e., isolated rotor) in hub-body system, ft/sec (m/sec)
$\Delta\dot{x},\Delta\dot{y},\Delta\dot{z}$	component of velocity at blade element due to aircraft motion in hub-body system, ft/sec (m/sec)
X_A,Y_A,Z_A	components of the total aerodynamic force on blade element in hub-body system, lb (N)
X_G,Y_G,Z_G	components of the gravitational force on blade element in hub-body system, lb (N)
α_r	blade element local angle of attack, rad (or deg)
ϕ_r	$\tan^{-1}(u_P/u_T)$, rad (or deg)
θ	blade pitch angle measured from hub plane, $\theta = \theta_o - A_{1s}\cos\psi - B_{1s}\sin\psi + \theta_{t,r} - K_1\beta - K_2\zeta$, rad (or deg)
θ_o	blade-root collective pitch measured from hub plane, rad (or deg)
$\theta_{t,r}$	blade twist at blade element, rad (or deg)
β	blade flapping angle measured from hub plane, rad (or deg)

$\dot{\beta}, \ddot{\beta}$	first and second derivative of β with respect to time
ζ	blade lagging angle (measured positive when opposite to the direction of rotor rotation), rad (or deg)
$\dot{\zeta}, \ddot{\zeta}$	first and second derivative of ζ with respect to time
ψ_a, θ_a, ϕ_a	Euler angles of the body-axis system with respect to the inertia system using the sequence of rotations as indicated
ρ	mass density of air, slug/ft^3 (kg/m^3)
Ω	rotor system angular velocity, rad/sec
ψ	azimuth angle measured from -x axis in the sense of rotor rotation, rad (or deg)

SUMMARY

This report documents a derivation of coupled flap-lag equations of motion for a rigid articulated rotor with hinge springs and viscous dampers. Three different flapping-lag-pitch hinge sequences are considered and the Lagrange method is used in deriving the equations. The effects of the complete six degrees-of-freedom aircraft motions are included and all the inertia dynamic terms are retained; no small-angle assumptions are used in the development. Comparisons of the results of this work with those available in the literature are made. Sources of terms missing in previous analyses, especially those of the inertia dynamics, are identified.

INTRODUCTION

Most helicopters in production today utilize articulated main rotors. A recent projection (ref. 1) indicates that, for the transport class of helicopters, future development may still rely heavily on the conventional articulated rotor design, although a trend seems to be set to use hingeless or bearingless rotors in the design of smaller combat helicopters to enhance agility and maintainability.

An articulated rotor uses flapping, lead-lag, and feathering hinges (or elastomeric bearings) in an appropriate sequence. The flapping hinge is employed to relieve the blade-root bending moment arising from the lift and centrifugal forces, the lag hinge to alleviate the in-plane moment at the blade root due to the drag force and the Coriolis force which stems from the flapping motion, and the feathering (or pitch) bearing to change the angle of attack of the blade. Figure 1 shows three widely used hinge sequences, i.e., flap-lag-pitch (F-L-P), flap-pitch-lag (F-P-L), and lag-flap-pitch (L-F-P) hinge arrangements. Use of a specific hinge sequence is often dictated by the past design experience and preference of the helicopter manufacturers. For example, Sikorsky designs tend to use an L-F-P hinge sequence with colocated hinges (refs. 2 and 3) as schematically shown in figure 2. The other two hinge sequences, the F-L-P and F-P-L, are more commonly used by other manufacturers.

The flap-lag equations of motion and the dynamic characteristics of the articulated rotor blades have been under intensive investigations for a long time (refs. 4-11), largely by rotor dynamicists, but it is only relatively recently that the importance of the hinge sequence has been recognized (refs. 8 and 9). The rotor dynamicists tend to place their main emphasis on the stability characteristics of the isolated rotor system and, as a consequence, will tend not to include the effects of aircraft (or shaft) motions (refs. 4-9). Therefore, the flap-lag

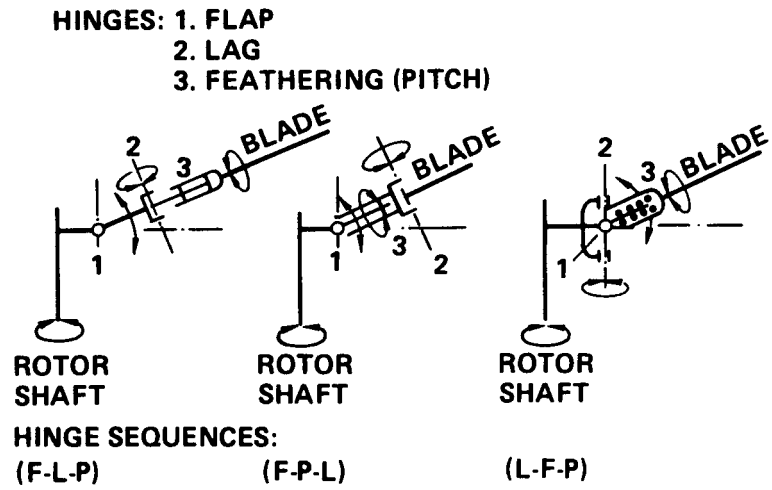

Figure 1.- Three commonly used hinge sequences (ref. 2).

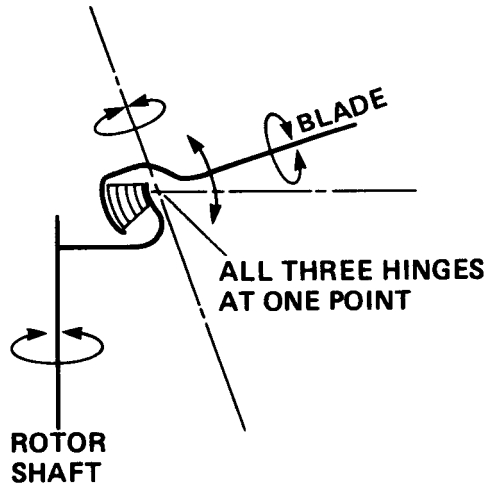

Figure 2.- Elastomeric-bearing rotor hub system (ref. 2).

equations of motion developed with this emphasis are not readily usable by the flight dynamicists, who are interested primarily in the stability and control characteristics of the entire vehicle and, as such, the effects of aircraft motions must be included in the development of flap-lag equations of motion. Some effects of aircraft motions were included, notably by the flight dynamicists (refs. 3, 10, and 11), but the effects are for specialized hinge arrangements. Extensions of those flap-lag equations of motion to include other hinge sequences and/or to include the complete effects of aircraft motion for a wider range of applications are not readily apparent, and therefore require a new development.

In the past, most rotor models developed expressly for flight dynamics and control applications, especially those for use in real-time simulation, have considered only the flapping motion (refs. 12-16). Recent studies related to high-bandwidth flight control systems for rotorcraft (refs. 17-21) have shown not only

that the flapping and other higher-order dynamics need to be considered (refs. 17-19), but the lead-lag dynamics must also be included in the rotor math model (refs. 20 and 21). These initial studies, coupled with the dramatically increased computational power that has become available in the past few years, serve as strong motivation to develop a generic rotor model for an articulated rotor system that includes various hinge arrangements for the rotor blades for a wider range of flight dynamics applications. It also permits a detailed investigation into the effects of hinge sequence.

The work reported here represents the first of a series of efforts designed to achieve the above objective. A detailed derivation is provided herein in the development of flap-lag equations of motion for the three commonly used hinge sequences, i.e., L-F-P, F-P-L, and F-L-P for articulated rigid blade with a complete account for the effects of aircraft motion.

COORDINATE SYSTEMS

In this section, the position and velocity of an element of a rotor blade are calculated. To express these vector quantities, the following coordinate systems are used. Different coordinate systems are used for the three hinge sequences considered.

L-F-P Hinge Sequence

Figure 3 shows the coordinate systems that are used for the L-F-P hinge sequence. The blade is assumed to be rigid. The pitch bearing is outboard of the flapping hinge, and the flapping hinge is outboard of the lag hinge.

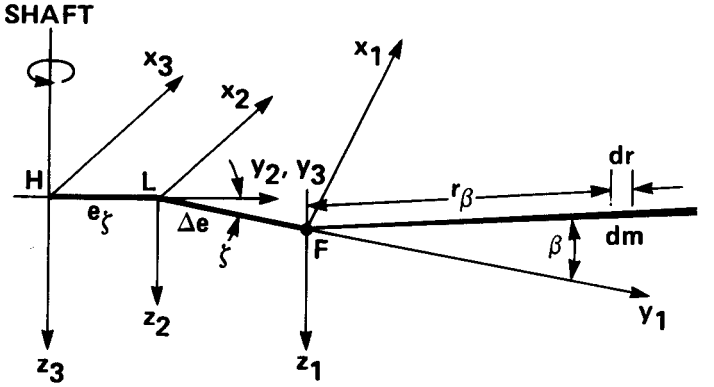

Figure 3.- Coordinate systems used for the L-F-P hinge sequence.

The flapping hinge is assumed to be perpendicular to the rotor shaft. The lag hinge is assumed to be parallel to the shaft. The feathering axis is assumed to

coincide with the blade span axis, and the center of gravity and aerodynamic pressure center of the blade sections are assumed to be on the blade span axis. With these assumptions in mind, the following coordinate systems are used:

x_1,y_1,z_1 - With its origin on the flapping hinge F; z_1 parallel to the shaft and pointing downward; y_1 parallel to the blade segment between the two hinges (coinciding with the feathering axis when flap angle is equal to zero) and pointing outward; z_1, y_1, and x_1 forming an orthogonal set.

x_2,y_2,z_2 - With origin on the lag hinge L; z_2 parallel to z_1; y_2 parallel to the blade segment between the shaft and L and pointing outward; z_2, y_2, and x_2 forming an orthogonal set.

x_3,y_3,z_3 - With origin at the hub center, otherwise the same as x_2,y_2,z_2 system. This coordinate system will be referred to as the rotating shaft system.

x,y,z - This axis system will be referred to as hub-body system with origin also at the hub center; z parallel to z_3; x pointing forward to the nose of the aircraft; y toward the right. This system is related to the rotating shaft system through the azimuth angle ψ as depicted in figure 4.

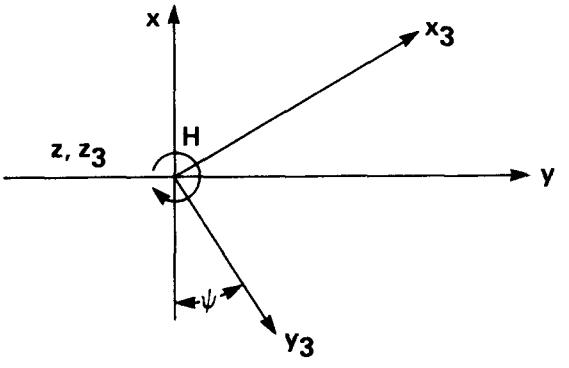

Figure 4.- Relationship of the rotating-shaft system and the hub-body system.

It is important to note that the sign convention regarding the flapping and lagging angles as defined in this report is: positive for flapping up and for lagging back. With this sign convention, the component of the position vector r with respect to the rotating-shaft and the hub-body systems are, respectively,

$$\begin{Bmatrix} x_3 \\ y_3 \\ z_3 \end{Bmatrix} = \begin{Bmatrix} 0 \\ e_\zeta \\ 0 \end{Bmatrix} + \begin{bmatrix} \cos\zeta & -\sin\zeta & 0 \\ \sin\zeta & \cos\zeta & 0 \\ 0 & 0 & 1 \end{bmatrix} \begin{Bmatrix} 0 \\ \Delta e + r_\beta \cos\beta \\ -r_\beta \sin\beta \end{Bmatrix}$$

$$= \begin{Bmatrix} -(\Delta e + r_\beta \cos\beta)\sin\zeta \\ e_\zeta + (\Delta e + r_\beta \cos\beta)\cos\zeta \\ -r_\beta \sin\beta \end{Bmatrix} \tag{1}$$

and

$$\begin{Bmatrix} x \\ y \\ z \end{Bmatrix} = \begin{bmatrix} \sin\psi & -\cos\psi & 0 \\ \cos\psi & \sin\psi & 0 \\ 0 & 0 & 1 \end{bmatrix} \begin{Bmatrix} x_3 \\ y_3 \\ z_3 \end{Bmatrix}$$

$$= \begin{Bmatrix} -(\Delta e + r_\beta \cos\beta)\sin\zeta \sin\psi - [e_\zeta + (\Delta e + r_\beta \cos\beta)\cos\zeta]\cos\psi \\ -(\Delta e + r_\beta \cos\beta)\sin\zeta \cos\psi + [e_\zeta + (\Delta e + r_\beta \cos\beta)\cos\zeta]\sin\psi \\ -r_\beta \sin\beta \end{Bmatrix} \tag{2}$$

The hub-body system is now related to the aircraft body-axis system (x_a, y_a, z_a) and an inertia system (x', y', z'). Figure 5 depicts the relationships among the three coordinate systems. Note that we consider a shaft tilt angle i, and a general offset of the hub center of the rotor system from the center of gravity of the aircraft (r_H). The center of gravity of the aircraft is translating (v_o), accelerating linearly (a_o), and rotating $(\omega, \dot{\omega})$ with respect to the inertia system. To expedite the development that follows, these vector quantities are now expressed in terms of the hub-body system, i.e.,

$$\begin{aligned} r &= (x,y,z)^T \\ r_H &= (\ell_x, \ell_y, \ell_z)^T \\ v_o &= (\dot{x}_o, \dot{y}_o, \dot{z}_o)^T \\ \omega &= (p,q,r)^T \end{aligned} \tag{3}$$

Note that when expressed in the hub-body system (also in the aircraft body-axis system), $a_o = (d/dt)(v_o) = (\partial/\partial t)(v_o) + \omega \times v_o$, and

$(d/dt)\omega = (\partial/\partial t)\omega + \omega \times \omega = (\partial/\partial t)\omega$, owing to the rotation of the system with respect to the inertia frame x',y',z'. Thus,

$$a_o = (a_x,a_y,a_z)^T = (\ddot{x}_o,\ddot{y}_o,\ddot{z}_o)^T + \begin{bmatrix} 0 & -r & q \\ r & 0 & -p \\ -q & p & 0 \end{bmatrix} (x,y,z)^T$$

$$\dot{\omega} = (\dot{p},\dot{q},\dot{r})^T$$

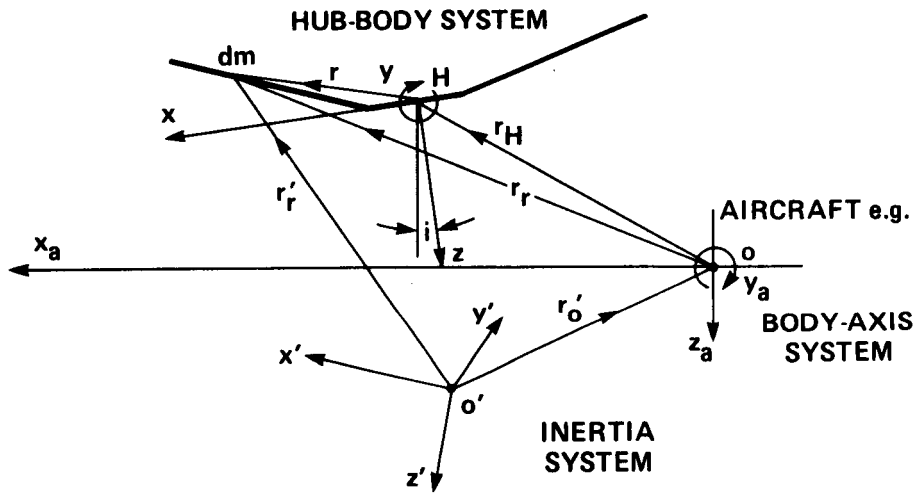

Figure 5.- Relationships among inertia, body-axis, and hub-body systems.

It should be noted that, due to the shaft tilt angle i, the components of the vector quantities in equation (3) differ from those which are expressed in the aircraft body-axis system by a transformation T_i,

$$T_i = \begin{bmatrix} \cos i & 0 & \sin i \\ 0 & 1 & 0 \\ -\sin i & 0 & \cos i \end{bmatrix} \tag{4a}$$

For example, if $v_o = (\dot{x}_a,\dot{y}_a,\dot{z}_a)^T$ and $\omega = (p_a,q_a,r_a)^T$ are, respectively, the linear velocity and angular velocity of the aircraft c.g. when expressed in the aircraft body-axis system, then in the hub-body system, $(\dot{x}_o,\dot{y}_o,\dot{z}_o)^T = T_i(\dot{x}_a,\dot{y}_a,\dot{z}_a)^T$ and $(p,q,r)^T = T_i(p_a,q_a,r_a)^T$. If the shaft has a sideward tilt with an angle j, in addition to the forward tilt angle i, then T_i is to be replaced by $T_{ji} = T_jT_i$, which is a result of the sequence of rotational transformations.

The aircraft body-axis system, x_a, y_a, z_a, is related to the inertia system, x', y', z', through the usual sequence of rotation of the Euler's angles, ψ_a, θ_a, ϕ_a. The components of a vector expressed in the two frames are related by the following transformation

$$\begin{Bmatrix} x_a \\ y_a \\ z_a \end{Bmatrix} = \begin{bmatrix} \cos\theta_a \cos\psi_a & \cos\theta_a \sin\psi_a & -\sin\theta_a \\ \sin\theta_a \sin\phi_a \cos\psi_a - \cos\phi_a \sin\psi_a & \sin\theta_a \sin\phi_a \sin\psi_a + \cos\phi_a \cos\psi_a & \sin\phi_a \cos\theta_a \\ \sin\theta_a \cos\phi_a \cos\psi_a + \sin\phi_a \sin\psi_a & \sin\theta_a \cos\phi_a \sin\psi_a - \sin\phi_a \cos\psi_a & \cos\theta_a \cos\phi_a \end{bmatrix} \begin{Bmatrix} x' \\ y' \\ z' \end{Bmatrix} \quad (4b)$$

From figure 5, it is clear that the sign convention for the components ℓ_x, ℓ_y, ℓ_z in equation (3) is as follows: ℓ_x is positive when the hub center H is forward of aircraft c.g. (along x-axis); ℓ_y is positive when H is to the right of c.g. (along y-axis); and ℓ_z is positive when H is below aircraft c.g. (along z-axis).

With the above considerations we are now in a position to determine the total velocity of the blade element.

Total velocity of blade element- With reference to figure 5, the position vector with respect to the aircraft c.g. is:

$$r_r = r_H + r$$

Expressed in the hub-body system, $r_r = (\ell_x + x, \ell_y + y, \ell_z + z)^T$, where $(x,y,z)^T$ are given in equation (2).

The total inertial velocity of the blade element V_r is (fig. 5):

$$V_r = \frac{d}{dt}(r'_r) = \frac{d}{dt}(r'_o) + \frac{d}{dt}(r_r)$$

$$= v_o + \frac{\partial}{\partial t}(r_r) + \omega \times r_r \quad (5)$$

Note that $(\partial/\partial t)(r_r) = (\partial/\partial t)(r)$, because $(\partial/\partial t)(r_H) = 0$. When expressed in the hub-body system, $(\partial/\partial t)(r)$ can be obtained by a simple differentiation of equation (2) with respect to time to yield

$$\frac{\partial}{\partial t}(r) = \begin{Bmatrix} \dot{x} \\ \dot{y} \\ \dot{z} \end{Bmatrix}$$

$$= \begin{Bmatrix} e_\zeta \Omega \sin\psi + r_\beta \dot{\beta} \sin\beta \cos(\psi - \zeta) + (\Delta e + r_\beta \cos\beta)(\Omega - \dot{\zeta})\sin(\psi - \zeta) \\ e_\zeta \Omega \cos\psi - r_\beta \dot{\beta} \sin\beta \sin(\psi - \zeta) + (\Delta e + r_\beta \cos\beta)(\Omega - \dot{\zeta})\cos(\psi - \zeta) \\ -r_\beta \dot{\beta} \cos\beta \end{Bmatrix} \tag{6}$$

The other terms on the right-hand side of equation (5) are due to aircraft motion

$$v_o + \omega \times r_r = \begin{Bmatrix} \dot{x}_o \\ \dot{y}_o \\ \dot{z}_o \end{Bmatrix} + \begin{bmatrix} 0 & -r & q \\ r & 0 & -p \\ -q & p & 0 \end{bmatrix} \begin{Bmatrix} \ell_x + x \\ \ell_y + y \\ \ell_z + z \end{Bmatrix} \tag{7a}$$

$$= \begin{Bmatrix} \dot{x}_o + qA - rB \\ \dot{y}_o - pA + rC \\ \dot{z}_o + pB - qC \end{Bmatrix} \tag{7b}$$

where from equation (2),

$$\left.\begin{aligned} A &= \ell_z - r_\beta \sin\beta \\ B &= (\ell_y + e_\zeta \sin\psi) + (\Delta e + r_\beta \cos\beta)\sin(\psi - \zeta) \\ C &= (\ell_x - e_\zeta \cos\psi) - (\Delta e + r_\beta \cos\beta)\cos(\psi - \zeta) \end{aligned}\right\} \tag{7c}$$

In the subsequent development, the velocity components of the blade element (eq. (7b)), which are due to aircraft motions, will be denoted by $(\Delta\dot{x},\Delta\dot{y},\Delta\dot{z})^T$. Equations (5), (6), and (7) thus completely define the total velocity components, in the hub-body system, of the blade element for the L-F-P hinge sequence. The coordinate systems used for the F-P-L hinge sequence are described next.

F-P-L Hinge Sequence

We now consider the second hinge sequence, F-P-L. With the pitch bearing in board of the lag hinge, the blade pitch motion couples directly to the lead-lag motion of the blade, because the feathering axis no longer passes through the blade-span axis. A sequence of coordinate systems, which differs from that used for the L-F-P hinge sequence previously discussed, is now set up as shown in figure 6. These coordinate systems have been previously used in reference 10 for a comprehensive flap-lag rotor analysis. That analysis was specifically for tandem rotor configurations. In order to apply the results of analysis to other rotorcraft configurations, such as side-by-side dual-rotor or tilt-rotor configurations, a more general analysis must be undertaken.

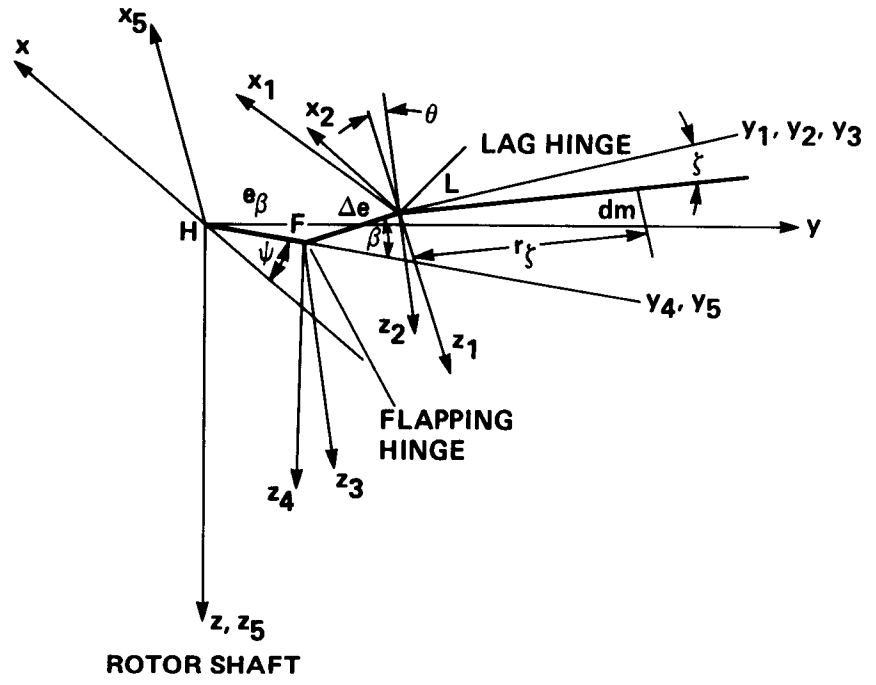

Figure 6.- Coordinate systems used for the F-P-L hinge sequence.

In figure 6, the x,y,z system is the hub-body system; the x_5,y_5,z_5 system is the rotating-shaft system (shown as x_3,y_3,z_3 in the L-F-P case); and the x_4,y_4,z_4 system is identical to the x_5,y_5,z_5 system except that its origin is now shifted from the hub center H to point F on the flapping hinge line, which is assumed to be in a direction perpendicular to the shaft. The x_3,y_3,z_3 system has its origin also located at F and is obtained by rotating about x_4 (thus $x_3 = x_4$) a flapping angle β so that y_3 aligns with FL. The x_2,y_2,z_2 system is obtained from x_3,y_3,z_3 system by shifting its origin from F to L on the lag hinge. Finally, the x_1,y_1,z_1 system is obtained from the x_2,y_2,z_2 system by a rotation θ about the y_2 axis. Now with respect to the x_1,y_1,z_1 system, the blade element dm has the components:

$$\begin{Bmatrix} x_1 \\ y_1 \\ z_1 \end{Bmatrix} = \begin{Bmatrix} -r_\zeta & \sin\zeta \\ r_\zeta & \cos\zeta \\ & 0 \end{Bmatrix} \tag{8}$$

With respect to the other coordinate systems, the components are obtained using the following transformations:

$$\begin{Bmatrix} x_2 \\ y_2 \\ z_2 \end{Bmatrix} = \begin{bmatrix} \cos\theta & 0 & \sin\theta \\ 0 & 1 & 0 \\ -\sin\theta & 0 & \cos\theta \end{bmatrix} \begin{Bmatrix} x_1 \\ y_1 \\ z_1 \end{Bmatrix} \tag{9}$$

$$\begin{Bmatrix} x_3 \\ y_3 \\ z_3 \end{Bmatrix} = \begin{Bmatrix} x_2 \\ y_2 + \Delta e \\ z_2 \end{Bmatrix} \tag{10}$$

$$\begin{Bmatrix} x_4 \\ y_4 \\ z_4 \end{Bmatrix} = \begin{bmatrix} 1 & 0 & 0 \\ 0 & \cos\beta & \sin\beta \\ 0 & -\sin\beta & \cos\beta \end{bmatrix} \begin{Bmatrix} x_3 \\ y_3 \\ z_3 \end{Bmatrix} \tag{11}$$

$$\begin{Bmatrix} x_5 \\ y_5 \\ z_5 \end{Bmatrix} = \begin{Bmatrix} x_4 \\ y_4 + e_\beta \\ z_4 \end{Bmatrix} \tag{12}$$

and

$$\begin{Bmatrix} x \\ y \\ z \end{Bmatrix} = \begin{bmatrix} \sin\psi & -\cos\psi & 0 \\ \cos\psi & \sin\psi & 0 \\ 0 & 0 & 1 \end{bmatrix} \begin{Bmatrix} x_5 \\ y_5 \\ z_5 \end{Bmatrix} \tag{13}$$

Combining equations (8) through (13), the components of the position vector r from the hub center H to the blade element dr (with mass dm as shown in fig. 6), when expressed in the hub-body system, are obtained:

$$r = \begin{Bmatrix} x \\ y \\ z \end{Bmatrix}$$

$$= \begin{Bmatrix} -(e_\beta + \Delta e \cos\beta + r_\zeta \cos\beta \cos\zeta + r_\zeta \sin\beta \sin\zeta \sin\theta)\cos\psi \\ \qquad\qquad - r_\zeta \cos\theta \sin\zeta \sin\psi \\ (e_\beta + \Delta e \cos\beta + r_\zeta \cos\beta \cos\zeta + r_\zeta \sin\beta \sin\zeta \sin\theta)\sin\psi \\ \qquad\qquad - r_\zeta \cos\theta \sin\zeta \cos\psi \\ -\Delta e \sin\beta - r_\zeta(\cos\zeta \sin\beta - \cos\beta \sin\zeta \sin\theta) \end{Bmatrix} \qquad (14)$$

Total velocity of the blade element- As in the case of the L-F-P hinge sequence, the total velocity of the blade element dr is the sum of the relative velocity of the blade element with respect to the hub center and the velocity caused by the aircraft motion as given in equation (5). The relative velocity with respect to the hub center, when expressed in the hub-body system, is obtained as before, that is, by directly taking the derivative of equation (14) with respect to time, yielding

$$\frac{\partial}{\partial t}(r) = \begin{Bmatrix} \dot{x} \\ \dot{y} \\ \dot{z} \end{Bmatrix} \qquad (15)$$

where

$$\dot{x} = \Omega[\sin\psi(e_\beta + r_\zeta \sin\beta \sin\zeta \sin\theta + \Delta e \cos\beta + r_\zeta \cos\beta \cos\zeta)$$
$$- r_\zeta \cos\psi \cos\theta \sin\zeta] + \dot{\beta} \cos\psi(r_\zeta \sin\beta \cos\zeta + \Delta e \sin\beta$$
$$- r_\zeta \cos\beta \sin\zeta \sin\theta) + \dot{\theta} r_\zeta \sin\zeta(\sin\psi \sin\theta - \cos\psi \sin\beta \cos\theta)$$
$$+ \dot{\zeta} r_\zeta(\cos\psi \cos\beta \sin\zeta - \sin\psi \cos\theta \cos\zeta - \cos\psi \sin\beta \cos\zeta \sin\theta)$$

$$\dot{y} = \Omega[\cos\psi(e_\beta + r_\zeta \sin\beta \sin\zeta \sin\theta + \Delta e \cos\beta + r_\zeta \cos\beta \cos\zeta)$$
$$+ r_\zeta \sin\psi \cos\theta \sin\zeta] + \dot{\beta} \sin\psi(-r_\zeta \sin\beta \cos\zeta - \Delta e \sin\beta \qquad (16)$$
$$+ r_\zeta \cos\beta \sin\zeta \sin\theta) + \dot{\theta} r_\zeta \sin\zeta(\cos\psi \sin\theta + \sin\psi \sin\beta \cos\theta)$$
$$+ \dot{\zeta} r_\zeta(-\sin\psi \cos\beta \sin\zeta - \cos\psi \cos\zeta \cos\theta + \sin\psi \sin\beta \cos\zeta \sin\theta)$$

$$\dot{z} = -\dot{\beta}(r_\zeta \cos\zeta \cos\beta + \Delta e \cos\beta + r_\zeta \sin\beta \sin\zeta \sin\theta)$$
$$+ \dot{\theta} r_\zeta(\cos\beta \sin\zeta \cos\theta) + \dot{\zeta} r_\zeta(\sin\zeta \sin\beta + \cos\beta \cos\zeta \sin\theta)$$

When expressed in the hub-body system, the components of the velocity of the blade element due to the aircraft motion is given in equation (7), in which the components of the position vector, $(x,y,z)^T$, are now given by equation (14) rather than equation (2). Denote these velocity components by $(\Delta\dot{x},\Delta\dot{y},\Delta\dot{z})^T$; then

$$v_o + \omega \times r_r = \begin{Bmatrix} \Delta\dot{x} \\ \Delta\dot{y} \\ \Delta\dot{z} \end{Bmatrix} \qquad (17a)$$

where

$$\Delta\dot{x} = \dot{x}_o + q\{\ell_z - \Delta e \sin\beta - r_\zeta(\cos\zeta \sin\beta - \cos\beta \sin\zeta \sin\theta)\}$$
$$- r\{\ell_y + [e_\beta + \Delta e \cos\beta + r_\zeta(\cos\beta \cos\zeta + \sin\beta \sin\zeta \sin\theta)]\sin\psi$$
$$- r_\zeta \cos\theta \sin\zeta \cos\psi\}$$

$$\Delta\dot{y} = \dot{y}_o + r\{\ell_x - [e_\beta + \Delta e \cos\beta + r_\zeta(\cos\beta \cos\zeta + \sin\beta \sin\zeta \sin\theta)]\cos\psi$$
$$- r_\zeta \cos\theta \sin\zeta \sin\psi\} - p\{\ell_z - \Delta e \sin\beta - r_\zeta(\cos\zeta \sin\beta \qquad (17b)$$
$$- \cos\beta \sin\zeta \sin\theta)\}$$

$$\Delta\dot{z} = \dot{z}_o - q\{\ell_x - [e_\beta + \Delta e \cos\beta + r_\zeta(\cos\beta \cos\zeta + \sin\beta \sin\zeta \sin\theta)]\cos\psi$$
$$- r_\zeta \cos\theta \sin\zeta \sin\psi\} + p\{\ell_y + [e_\beta + \Delta e \cos\beta + r_\zeta(\cos\beta \cos\zeta$$
$$+ \sin\beta \sin\zeta \sin\theta)]\sin\psi - r_\zeta \cos\theta \sin\zeta \cos\psi\}$$

and the components of the total velocity of the blade element are the sum of equations (16) and (17), i.e.,

$$V_r = \begin{Bmatrix} \dot{x} + \Delta\dot{x} \\ \dot{y} + \Delta\dot{y} \\ \dot{z} + \Delta\dot{z} \end{Bmatrix} \qquad (18)$$

This completes the determination of the position and velocity components of the blade element in the hub-body system for the F-P-L hinge sequence.

F-L-P Hinge Sequence

The position and velocity of the blade element for the F-L-P hinge sequence can be obtained directly from those for the F-P-L hinge sequence by omitting the transformation caused by blade pitch rotation. Setting $\theta = 0$ in equation (14) yields the position components in the hub-body system:

$$r = \begin{Bmatrix} x \\ y \\ z \end{Bmatrix} = \begin{Bmatrix} -(e_\beta + \Delta e \cos\beta + r_\zeta \cos\beta \cos\zeta)\cos\psi - r_\zeta \sin\zeta \sin\psi \\ (e_\beta + \Delta e \cos\beta + r_\zeta \cos\beta \cos\zeta)\sin\psi - r_\zeta \sin\zeta \cos\psi \\ -(\Delta e + r_\zeta \cos\zeta)\sin\beta \end{Bmatrix} \qquad (19)$$

Likewise, the total velocity of the blade element is obtained by setting $\theta = \dot{\theta} = 0$ in equations (16) and (17b) to yield:

$$V_r = \begin{Bmatrix} \dot{x} + \Delta\dot{x} \\ \dot{y} + \Delta\dot{y} \\ \dot{z} + \Delta\dot{z} \end{Bmatrix} \tag{20a}$$

where

$$\dot{x} = \Omega[\sin\psi(e_\beta + \Delta e\cos\beta + r_\zeta\cos\beta\cos\zeta) - r_\zeta\cos\psi\sin\zeta]$$
$$+ \dot{\beta}\cos\psi\sin\beta(\Delta e + r_\zeta\cos\zeta) + \dot{\zeta}r_\zeta(\cos\psi\cos\beta\sin\zeta - \sin\psi\cos\zeta)$$

$$\dot{y} = \Omega[\cos\psi(e_\beta + \Delta e\cos\beta + r_\zeta\cos\beta\cos\zeta) + r_\zeta\sin\psi\sin\zeta]$$
$$- \dot{\beta}\sin\psi\sin\beta(\Delta e + r_\zeta\cos\zeta) - \dot{\zeta}r_\zeta(\sin\psi\cos\beta\sin\zeta + \cos\psi\cos\zeta)$$

$$\dot{z} = -\dot{\beta}\cos\beta(\Delta e + r_\zeta\cos\zeta) + \dot{\zeta}r_\zeta\sin\zeta\sin\beta$$

and

$$\Delta\dot{x} = \dot{x}_o + q\{\ell_z - (\Delta e + r_\zeta\cos\zeta)\sin\beta\}$$
$$- r\{\ell_y + [e_\beta + (\Delta e + r_\zeta\cos\zeta)\cos\beta]\sin\psi - r_\zeta\cos\psi\sin\zeta\}$$

$$\Delta\dot{y} = \dot{y}_o + r\{\ell_x - [e_\beta + (\Delta e + r_\zeta\cos\zeta)\cos\beta]\cos\psi - r_\zeta\sin\psi\sin\zeta\}$$
$$- p\{\ell_z - (\Delta e + r_\zeta\cos\zeta)\sin\beta\} \tag{20b}$$

$$\Delta\dot{z} = \dot{z}_o - q\{\ell_x - [e_\beta + (\Delta e + r_\zeta\cos\zeta)\cos\beta]\cos\psi - r_\zeta\sin\psi\sin\zeta\}$$
$$+ p\{\ell_y + [e_\beta + (\Delta e + r_\zeta\cos\zeta)\cos\beta]\sin\psi - r_\zeta\cos\psi\sin\zeta\}$$

This concludes the derivation for the expressions of the position and velocity components of the blade element, in the hub-body system, for the F-L-P hinge sequence.

The total velocity as given in equations (5), (18), and (20), respectively, for L-F-P, F-P-L, and F-L-P hinge sequences is required for developing the coupled flap-lag equations of motion using the Lagrange method. It is also required for the calculation of the aerodynamic forces and moments to be discussed later in this

report. The development of the flapping and lag equations is given in the next section.

INERTIA DYNAMICS

The Lagrangian procedure is applied to develop the inertia dynamics for the flapping and lag motion. This procedure begins with the determination of the kinetic energy of a single blade. This is obtained by integrating the kinetic energy of the blade element over the entire blade span. The development of flap/lag equations of motion will be given separately for each of the three hinge sequences.

L-F-P Hinge Sequence

The kinetic energy of the single rotor blade is determined by summing up that for each blade element, $(1/2)V_r \cdot V_r \, dm$, over the entire blade span, i.e.,

$$T = 1/2 \int_o^R V_r \cdot V_r \, dm \tag{21}$$

To help identify the contribution of the aircraft motion to the total kinetic energy, the dot product of the total velocity, $V_r \cdot V_r$, will be expressed in the following manner:

$$V_r \cdot V_r = (\dot{x} + \Delta\dot{x})^2 + (\dot{y} + \Delta\dot{y})^2 + (\dot{z} + \Delta\dot{z})^2$$

$$= (\dot{x}^2 + \dot{y}^2 + \dot{z}^2) + \Delta\dot{x}^2 + \Delta\dot{y}^2 + \Delta\dot{z}^2 + 2(\Delta\dot{x}\dot{x} + \Delta\dot{y}\dot{y} + \Delta\dot{z}\dot{z}) \tag{22}$$

The first term of the right-hand side of equation (22) involves no effects of aircraft motion and it can be calculated directly from equation (6); the remaining terms involve the effects of aircraft motion and are determined using equations (6) and (7). The result is

$$\begin{aligned} V_r \cdot V_r = {} & e_\zeta^2\Omega^2 + r_\beta^2\dot{\beta}^2 + (\Delta e + r_\beta \cos\beta)^2(\Omega - \dot{\zeta})^2 + 2e_\zeta\Omega[r_\beta\dot{\beta}\sin\beta\sin\zeta \\ & + (\Delta e + r_\beta\cos\beta)(\Omega - \dot{\zeta})\cos\zeta] + (\dot{x}_o^2 + \dot{y}_o^2 + \dot{z}_o^2) \\ & + 2(q\dot{x}_o - p\dot{y}_o)(\ell_z - r_\beta\sin\beta) + 2r\{\dot{y}_o[(\ell_x - e_\zeta\cos\psi) \\ & - (\Delta e + r_\beta\cos\beta)\cos(\psi - \zeta)] - \dot{x}_o[(\ell_y + e_\zeta\sin\psi) \\ & + (\Delta e + r_\beta\cos\beta)\sin(\psi - \zeta)]\} + 2\dot{z}_o\{p[(\ell_y + e_\zeta\sin\psi) \\ & + (\Delta e + r_\beta\cos\beta)\sin(\psi - \zeta)] - q[(\ell_x - e_\zeta\cos\psi) \end{aligned}$$

$$
\begin{aligned}
&- (\Delta e + r_\beta \cos\beta)\cos(\psi - \zeta)]\} + 2\{\dot{x}_o[e_\zeta \Omega \sin\psi + r_\beta \dot{\beta} \sin\beta \cos(\psi - \zeta) \\
&+ (\Delta e + r_\beta \cos\beta)(\Omega - \dot{\zeta})\sin(\psi - \zeta)] + \dot{y}_o[e_\zeta \Omega \cos\psi \\
&- r_\beta \dot{\beta} \sin\beta \sin(\psi - \zeta) + (\Delta e + r_\beta \cos\beta)(\Omega - \dot{\zeta})\cos(\psi - \zeta)] \\
&- \dot{z}_o r_\beta \dot{\beta} \cos\beta\} + (p^2 + q^2)(\ell_z - r_\beta \sin\beta)^2 \\
&+ (p^2 + r^2)[(\ell_y + e_\zeta \sin\psi) + (\Delta e + r_\beta \cos\beta)\sin(\psi - \zeta)]^2 \\
&+ (r^2 + q^2)[(\ell_x - e_\zeta \cos\psi) - (\Delta e + r_\beta \cos\beta)\cos(\psi - \zeta)]^2 \\
&- 2r(\ell_z - r_\beta \sin\beta)\{q[(\ell_y + e_\zeta \sin\psi) + (\Delta e + r_\beta \cos\beta)\sin(\psi - \zeta)] \\
&+ p[(\ell_x - e_\zeta \cos\psi) - (\Delta e + r_\beta \cos\beta)\cos(\psi - \zeta)]\} \\
&- 2pq[(\ell_y + e_\zeta \sin\psi) + (\Delta e + r_\beta \cos\beta)\sin(\psi - \zeta)][(\ell_x - e_\zeta \cos\psi) \\
&- (\Delta e + r_\beta \cos\beta)\cos(\psi - \zeta)] + 2(\ell_z - r_\beta \sin\beta)\{q[e_\zeta \Omega \sin\psi \\
&+ r_\beta \dot{\beta} \sin\beta \cos(\psi - \zeta) + (\Delta e + r_\beta \cos\beta)(\Omega - \dot{\zeta})\sin(\psi - \zeta)] \\
&- p[e_\zeta \Omega \cos\psi - r_\beta \dot{\beta} \sin\beta \sin(\psi - \zeta) \\
&+ (\Delta e + r_\beta \cos\beta)(\Omega - \dot{\zeta})\cos(\psi - \zeta)]\} - 2r_\beta \dot{\beta} \cos\beta\{p[(\ell_y + e_\zeta \sin\psi) \\
&+ (\Delta e + r_\beta \cos\beta)\sin(\psi - \zeta) - q[(\ell_x - e_\zeta \cos\psi) \\
&- (\Delta e + r_\beta \cos\beta)\cos(\psi - \zeta)]\} + 2r\{[(\ell_x - e_\zeta \cos\psi) \\
&- (\Delta e + r_\beta \cos\beta)\cos(\psi - \zeta)][e_\zeta \Omega \cos\psi - r_\beta \dot{\beta} \sin\beta \sin(\psi - \zeta) \\
&+ (\Delta e + r_\beta \cos\beta)(\Omega - \dot{\zeta})\cos(\psi - \zeta)] - [(\ell_y + e_\zeta \sin\psi) \\
&+ (\Delta e + r_\beta \cos\beta)\sin(\psi - \zeta)][e_\zeta \Omega \sin\psi + r_\beta \dot{\beta} \sin\beta \cos(\psi - \zeta) \\
&+ (\Delta e + r_\beta \cos\beta)(\Omega - \dot{\zeta})\sin(\psi - \zeta)]\} \qquad (23)
\end{aligned}
$$

The zeroth, first, and second mass moments of the blade segment outside the flapping hinge are denoted by

$$
I_\beta = \int_o^R r_\beta^2 \, dm \,, \quad M_\beta = \int_o^R r_\beta \, dm \,, \quad \text{and} \quad m_\beta = \int_o^R dm
$$

in which the limits of integration are from the flapping hinge to the tip of the blade. Consideration of the kinetic energy associated with the blade segment inboard of the flapping hinge introduces additional terms. Appendix A discusses the impact of this on the inertia dynamics for the three hinge sequences considered. The kinetic energy associated with a single rotor blade, T, is determined to be

$$
\begin{aligned}
T = \frac{1}{2}\{&\dot{\beta}^2 I_\beta + \dot{\zeta}^2(\Delta e^2 m_\beta + 2\Delta e M_\beta \cos\beta + I_\beta \cos^2\beta) + \Omega^2[(e_\zeta^2 + \Delta e^2)m_\beta \\
&+ 2\Delta e M_\beta \cos\beta + I_\beta \cos^2\beta] + 2\Omega^2 e_\zeta(\Delta e m_\beta + M_\beta \cos\beta)\cos\zeta \\
&- 2\dot{\zeta}\Omega[e_\zeta(\Delta e m_\beta + M_\beta \cos\beta)\cos\zeta + (\Delta e^2 m_\beta + 2\Delta e M_\beta \cos\beta + I_\beta \cos^2\beta)] \\
&+ 2\dot{\beta}\Omega e_\zeta M_\beta \sin\beta \sin\zeta\} + \frac{1}{2}(\dot{x}_o^2 + \dot{y}_o^2 + \dot{z}_o^2)m_\beta + (q\dot{x}_o - p\dot{y}_o)(\ell_z m_\beta - M_\beta \sin\beta) \\
&+ r\{\dot{y}_o[(\ell_x - e_\zeta \cos\psi)m_\beta - (\Delta e m_\beta + M_\beta \cos\beta)\cos(\psi - \zeta)] \\
&- \dot{x}_o[(\ell_y + e_\zeta \sin\psi)m_\beta + (\Delta e m_\beta + M_\beta \cos\beta)\sin(\psi - \zeta)]\} \\
&+ \dot{z}_o\{p[\ell_y + e_\zeta \sin\psi)m_\beta + (\Delta e m_\beta + M_\beta \cos\beta)\sin(\psi - \zeta) - q[(\ell_x - e_\zeta \cos\psi)m_\beta \\
&- (\Delta e m_\beta + M_\beta \cos\beta)\cos(\psi - \zeta)]\} + \dot{x}_o[e_\zeta m_\beta \Omega \sin\psi + M_\beta \dot{\beta} \sin\beta \cos(\psi - \zeta) \\
&+ (\Delta e m_\beta + M_\beta \cos\beta)(\Omega - \dot{\zeta})\sin(\psi - \zeta)] + \dot{y}_o[e_\zeta m_\beta \Omega \cos\psi \\
&- M_\beta \dot{\beta} \sin\beta \sin(\psi - \zeta) + (\Delta e m_\beta + M_\beta \cos\beta)(\Omega - \dot{\zeta})\cos(\psi - \zeta)] - \dot{z}_o M_\beta \dot{\beta} \cos\beta \\
&+ \frac{1}{2}(p^2 + q^2)(\ell_z^2 m_\beta - 2\ell_z M_\beta \sin\beta + I_\beta \sin^2\beta) \\
&+ \frac{1}{2}(p^2 + r^2)[(\ell_y + e_\zeta \sin\psi)^2 m_\beta \\
&+ 2(\ell_y + e_\zeta \sin\psi)(\Delta e m_\beta + M_\beta \cos\beta)\sin(\psi - \zeta) \\
&+ (\Delta e^2 m_\beta + 2\Delta e M_\beta \cos\beta + I_\beta \cos^2\beta)\sin^2(\psi - \zeta)] \\
&+ \frac{1}{2}(q^2 + r^2)[(\ell_x - e_\zeta \cos\psi)^2 m_\beta \\
&- 2(\ell_x - e_\zeta \cos\psi)(\Delta e m_\beta + M_\beta \cos\beta)\cos(\psi - \zeta) \\
&+ (\Delta e^2 m_\beta + 2\Delta e M_\beta \cos\beta + I_\beta \cos^2\beta)\cos^2(\psi - \zeta)] \\
&- pq[(\ell_y + e_\zeta \sin\psi)(\ell_x - e_\zeta \cos\psi)m_\beta \\
&- (\ell_y + e_\zeta \sin\psi)(\Delta e m_\beta + M_\beta \cos\beta)\cos(\psi - \zeta) \\
&+ (\ell_x - e_\zeta \cos\psi)(\Delta e m_\beta + M_\beta \cos\beta)\sin(\psi - \zeta) \\
&- (\Delta e^2 m_\beta + 2\Delta e M_\beta \cos\beta + I_\beta \cos^2\beta)\sin(\psi - \zeta)\cos(\psi - \zeta)]
\end{aligned}
$$

$$
\begin{aligned}
&- pr\{(\ell_x - e_\zeta \cos\psi)(\ell_z m_\beta - M_\beta \sin\beta) - [\ell_z(\Delta e m_\beta + M_\beta \cos\beta) \\
&- \Delta e M_\beta \sin\beta - I_\beta \sin\beta\cos\beta]\cos(\psi - \zeta)\} \\
&- qr\{(\ell_y + e_\zeta \sin\psi)(\ell_z m_\beta - M_\beta \sin\beta) \\
&+ [\ell_z(\Delta e m_\beta + M_\beta \cos\beta) - \Delta e M_\beta \sin\beta - I_\beta \sin\beta\cos\beta]\sin(\psi - \zeta)\} \\
&+ (\ell_z m_\beta - M_\beta \sin\beta)\{q[e_\zeta \Omega \sin\psi + \Delta e(\Omega - \dot{\zeta})\sin(\psi - \zeta)] \\
&- p[e_\zeta \Omega \cos\psi + \Delta e(\Omega - \dot{\zeta})\cos(\psi - \zeta)]\} \\
&+ (\ell_z M_\beta - I_\beta \sin\beta)\{q[\dot{\beta}\sin\beta\cos(\psi - \zeta) + (\Omega - \dot{\zeta})\cos\beta\sin(\psi - \zeta)] \\
&+ p[\dot{\beta}\sin\beta\sin(\psi - \zeta) - (\Omega - \dot{\zeta})\cos\beta\cos(\psi - \zeta)]\} \\
&- \dot{\beta}\cos\beta\{p[(\ell_y + e_\zeta \sin\psi)M_\beta + (\Delta e M_\beta + I_\beta \cos\beta)\sin(\psi - \zeta) \\
&- q[(\ell_x - e_\zeta \cos\psi)M_\beta - (\Delta e M_\beta + I_\beta \cos\beta)\cos(\psi - \zeta)]\} \\
&+ r\{(\ell_x - e_\zeta \cos\psi)[m_\beta e_\zeta \Omega \cos\psi - M_\beta \dot{\beta}\sin\beta\sin(\psi - \zeta) \\
&+ (\Delta e m_\beta + M_\beta \cos\beta)(\Omega - \dot{\zeta})\cos(\psi - \zeta)] \\
&- (\ell_y + e_\zeta \sin\psi)[m_\beta e_\zeta \Omega \sin\psi + M_\beta \dot{\beta}\sin\beta\cos(\psi - \zeta) \\
&+ (\Delta e m_\beta + M_\beta \cos\beta)(\Omega - \dot{\zeta})\sin(\psi - \zeta)] - (\Delta e m_\beta + M_\beta \cos\beta)e_\zeta \Omega \cos\zeta \\
&- (\Delta e^2 m_\beta + 2\Delta e M_\beta \cos\beta + I_\beta \cos^2\beta)(\Omega - \dot{\zeta})\}
\end{aligned}
\tag{24}
$$

It can be seen from equation (24) that the aircraft motion greatly complicates the expression for the kinetic energy of the rotor blade. It also complicates, as can be expected, the equations of motion of the blade.

The coupled flap-lag equations of motion are now derived using the Lagrange procedure (refs. 22 and 23). They are calculated using

$$\frac{d}{dt}\left(\frac{\partial T}{\partial \dot{\zeta}}\right) - \frac{\partial T}{\partial \zeta} = Q_\zeta \tag{25a}$$

$$\frac{d}{dt}\left(\frac{\partial T}{\partial \dot{\beta}}\right) - \frac{\partial T}{\partial \beta} = Q_\beta \tag{25b}$$

In equations (25a) and (25b), Q_ζ and Q_β are the generalized forces (moments in the present case). They consist of the effects due to gravity, aerodynamic forces, and

the forces due to lag dampers and hinge springs. These will be discussed later in this report.

Coupled flap-lag equations of motion- With some algebraic manipulations of equations (24) and (25a) the lag equation of motion becomes:

$$\begin{aligned}
&\ddot{\zeta}(\Delta e^2 m_\beta + 2\Delta e M_\beta \cos\beta + I_\beta \cos^2\beta) \\
&= \dot{\Omega}(\Delta e^2 m_\beta + 2\Delta e M_\beta \cos\beta + I_\beta \cos^2\beta) + (\Delta e m_\beta + M_\beta \cos\beta)\{a_x \sin(\psi - \zeta) \\
&\quad + a_y \cos(\psi - \zeta) + e[(\dot{\Omega} - \dot{r})\cos\zeta - (\Omega - r)^2 \sin\zeta - pq\cos(2\psi - \zeta) \\
&\quad - p^2 \sin\psi \cos(\psi - \zeta) + q^2 \cos\psi \sin(\psi - \zeta)] - \Delta e[\dot{r} + pq\cos 2(\psi - \zeta) \\
&\quad + \tfrac{1}{2}(p^2 - q^2)\sin 2(\psi - \zeta)] + \ell_x[(\dot{r} + pq)\cos(\psi - \zeta) - (q^2 + r^2)\sin(\psi - \zeta)] \\
&\quad + \ell_y[(pq - \dot{r})\sin(\psi - \zeta) - (p^2 + r^2)\cos(\psi - \zeta)] \\
&\quad - \ell_z[(\dot{p} - qr)\cos(\psi - \zeta) - (\dot{q} + pr)\sin(\psi - \zeta)]\} \\
&\quad + (\Delta e M_\beta + I_\beta \cos\beta)\{\sin\beta[2\dot{\beta}(r - \Omega + \dot{\zeta}) + (\dot{p} - qr)\cos(\psi - \zeta) \\
&\quad - (\dot{q} + pr)\sin(\psi - \zeta)] - \cos\beta\{\dot{r} + pq\cos 2(\psi - \zeta) + \tfrac{1}{2}(p^2 - q^2)\sin 2(\psi - \zeta) \\
&\quad - 2\dot{\beta}[p\cos(\psi - \zeta) - q\sin(\psi - \zeta)]\}\} + Q_{\zeta_1}
\end{aligned} \tag{26}$$

Similarly, from equations (24) and (25b), the flapping equation of motion is obtained:

$$\begin{aligned}
\ddot{\beta} = \frac{M_\beta}{I_\beta}\{&\sin\beta\{a_y \sin(\psi - \zeta) - a_x \cos(\psi - \zeta) - e[\dot{\Omega}\sin\zeta + (\Omega^2 - 2r\Omega)\cos\zeta] \\
&- \Delta e[(\Omega - \dot{\zeta})^2 - 2r(\Omega - \dot{\zeta})] \\
&+ [\ell_x - e_\zeta \cos\psi - \Delta e\cos(\psi - \zeta)][(\dot{r} + pq)\sin(\psi - \zeta) + (q^2 + r^2)\cos(\psi - \zeta)] \\
&+ [\ell_y + e_\zeta \sin\psi + \Delta e\sin(\psi - \zeta)][(\dot{r} - pq)\cos(\psi - \zeta) - (p^2 + r^2)\sin(\psi - \zeta)] \\
&- \ell_z[(\dot{p} - qr)\sin(\psi - \zeta) + (\dot{q} + pr)\cos(\psi - \zeta)]\} \\
&+ \cos\beta\{a_z + 2p[\Omega e_\zeta \cos\psi + \Delta e(\Omega - \dot{\zeta})\cos(\psi - \zeta)] \\
&- 2q[\Omega e_\zeta \sin\psi + \Delta e(\Omega - \dot{\zeta})\sin(\psi - \zeta)] \\
&- (\dot{q} - pr)[\ell_x - e_\zeta \cos\psi - \Delta e\cos(\psi - \zeta)] \\
&+ (\dot{p} + qr)[\ell_y + e_\zeta \sin\psi + \Delta e\sin(\psi - \zeta)] - (p^2 + q^2)\ell_z\}\}
\end{aligned}$$

$$+ \sin\beta\{[(\dot{p} - qr)\sin(\psi - \zeta) + (\dot{q} + pr)\cos(\psi - \zeta)]\sin\beta$$

$$- \{[p\sin(\psi - \zeta) + q\cos(\psi - \zeta)]^2 + [r - (\Omega - \dot{\zeta})]^2\}\cos\beta\}$$

$$+ \cos\beta\{(p^2 + q^2)\sin\beta + \{2(\Omega - \dot{\zeta})[p\cos(\psi - \zeta) - q\sin(\psi - \zeta)]$$

$$+ (\dot{p} + qr)\sin(\psi - \zeta) + (\dot{q} - pr)\cos(\psi - \zeta)\}\cos\beta\} + \frac{Q_{\beta_1}}{I_\beta} \qquad (27)$$

In equations (26) and (27), a_x, a_y, and a_z are, respectively, the components of the total linear acceleration at the aircraft c.g. when projected along the x,y,z axes of the hub-body system. It is important to recognize that these components are different from $\ddot{x}_o$, $\ddot{y}_o$, and $\ddot{z}_o$, which are obtained by differentiating $\dot{x}_o$, $\dot{y}_o$, and $\dot{z}_o$ with respect to time, without considering the fact that the hub-body system is rotating about the inertia system, x',y',z'. In fact, from equation (3),

$$a_x = \ddot{x}_o - r\dot{y}_o + q\dot{z}_o \qquad (28a)$$

$$a_y = \ddot{y}_o + r\dot{x}_o - p\dot{z}_o \qquad (28b)$$

$$a_z = \ddot{z}_o + p\dot{y}_o - q\dot{x}_o \qquad (28c)$$

This distinction becomes particularly important when combining the flap-lag equations with the rigid-body aircraft equations of motion to calculate the dynamics and responses of the complete rotorcraft.

Equations (26) and (27) are the coupled flap-lag equations of motion for the L-F-P hinge sequence. It should be noted that in deriving these equations, the inertial effects of the blade segment inboard of the flapping hinge were neglected. When these effects are included, the inertia dynamic terms in the lag equation (26) must be expanded to include additional terms given by equation (A2) in appendix A. However, the flapping equation (27) remains unchanged, because they have no direct effect on the flapping motion.

F-P-L Hinge Sequence

The coupled flap-lag equations of motion for the F-P-L hinge sequence are developed in the same manner as for the L-F-P hinge sequence discussed previously. Using equations (16), (17b), (21), (22), (25a), and (25b), the coupled flap-lag equations of motion are obtained:

$$
\begin{aligned}
I_\zeta \ddot{\zeta} = {} & \ddot{\beta} \sin\theta (I_\zeta + \Delta e M_\zeta \cos\zeta) + \dot{\Omega} \cos\theta [I_\zeta \cos\beta + M_\zeta \cos\zeta (e_\beta + \Delta e \cos\beta)] \\
& + 2\dot{\beta}\dot{\theta} I_\zeta \cos\theta \sin^2\zeta \\
& - 2\Omega\dot{\beta} \cos\theta \cos\zeta [I_\zeta (\sin\beta \cos\zeta - \cos\beta \sin\zeta \sin\theta) + \Delta e M_\zeta \sin\beta] \\
& + 2\Omega\dot{\theta} \sin\zeta I_\zeta (\sin\beta \cos\zeta - \cos\beta \sin\zeta \sin\theta) + \dot{\theta}^2 I_\zeta \sin\zeta \cos\zeta \\
& - \dot{\beta}^2 \sin\zeta (I_\zeta \cos\zeta \cos^2\theta + \Delta e M_\zeta) \\
& + \Omega^2 \Big\{ I_\zeta \Big[\tfrac{1}{2} \sin 2\zeta (\sin^2\beta - \cos^2\beta \sin^2\theta) + \cos 2\zeta \sin\beta \cos\beta \sin\theta \Big] \\
& + (e_\beta M_\zeta + \Delta e M_\zeta \cos\beta)(\sin\beta \cos\zeta \sin\theta - \cos\beta \sin\zeta) \Big\} \\
& + M_\zeta [a_x (\cos\zeta \sin\psi \cos\theta + \cos\zeta \cos\psi \sin\theta \sin\beta - \sin\zeta \cos\psi \cos\beta) \\
& + a_y (\cos\zeta \cos\psi \cos\theta - \cos\zeta \sin\psi \sin\theta \sin\beta + \sin\zeta \sin\psi \cos\beta) \\
& - a_z (\cos\zeta \sin\theta \cos\beta + \sin\zeta \sin\beta)] \\
& + 2\dot{\theta} I_\zeta \{ \sin\zeta \cos\zeta (q \sin\psi \cos\beta - p \cos\psi \cos\beta - r \sin\beta) \\
& + \sin^2\zeta [\sin\theta (q \sin\psi \sin\beta - p \cos\psi \sin\beta + r \cos\beta) \\
& - \cos\theta (q \cos\psi + p \sin\psi)] \} \\
& + 2\dot{\beta} [(I_\zeta \cos\zeta \cos^2\theta + \Delta e M_\zeta) \sin\zeta (q \cos\psi + p \sin\psi) \\
& - (I_\zeta \cos\zeta + \Delta e M_\zeta) \cos\zeta \cos\theta (q \sin\psi \cos\beta - p \cos\psi \cos\beta - r \sin\beta) \\
& - I_\zeta \cos\theta \sin\theta \cos\zeta \sin\zeta (q \sin\psi \sin\beta - p \cos\psi \sin\beta + r \cos\beta)] \\
& + 2\Omega \{ [(e_\beta M_\zeta + \Delta e M_\zeta \cos\beta) + I_\zeta (\cos\beta \cos\zeta + \sin\beta \sin\zeta \sin\theta)] \\
& \times [\sin\theta \cos\zeta (q \sin\psi \cos\beta - p \cos\psi \cos\beta - r \sin\beta) \\
& + \sin\zeta (q \sin\psi \sin\beta - p \cos\psi \sin\beta + r \cos\beta)] \\
& - I_\zeta \cos\theta \sin\zeta [(\sin\theta \cos\zeta \cos\beta + \sin\zeta \sin\beta)(q \cos\psi + p \sin\psi) \\
& + r \cos\zeta \cos\theta] \} + \{ M_\zeta [-\ell_x + (e_\beta + \Delta e \cos\beta) \cos\psi] \\
& + I_\zeta [\sin\psi \cos\theta \sin\zeta + \cos\psi (\cos\beta \cos\zeta + \sin\beta \sin\zeta \sin\theta)] \} \\
& \times \{ \sin\theta \cos\zeta [(q^2 + r^2) \cos\psi \sin\beta + (pq + \dot{r}) \sin\psi \sin\beta - (\dot{q} - pr) \cos\beta] \\
& - \sin\zeta [(q^2 + r^2) \cos\psi \cos\beta + (pq + \dot{r}) \sin\psi \cos\beta + (\dot{q} - pr) \sin\beta]
\end{aligned}
$$

$$+ \cos\zeta\cos\theta[(q^2 + r^2)\sin\psi - (pq + \dot{r})\cos\psi]\}$$

$$+ \{M_\zeta[\ell_y + (e_\beta + \Delta e\cos\beta)\sin\psi]$$

$$+ I_\zeta[-\cos\theta\sin\zeta\cos\psi + \sin\psi(\cos\beta\cos\zeta + \sin\beta\sin\zeta\sin\theta)]\}$$

$$\times \{\sin\theta\cos\zeta[(pq - \dot{r})\cos\psi\sin\beta + (p^2 + r^2)\sin\psi\sin\beta - (\dot{p} + qr)\cos\beta]$$

$$- \sin\zeta[(pq - \dot{r})\cos\psi\cos\beta + (p^2 + r^2)\sin\psi\cos\beta + (\dot{p} + qr)\sin\beta]$$

$$+ \cos\theta\cos\zeta[(pq - \dot{r})\sin\psi - (p^2 + r^2)\cos\psi]\}$$

$$+ \{M_\zeta(-\ell_z + \Delta e\sin\beta) + I_\zeta(\sin\beta\cos\zeta - \cos\beta\sin\zeta\sin\theta)\}$$

$$\times \{\sin\theta\cos\zeta[-(\dot{q} + pr)\cos\psi\sin\beta - (\dot{p} - qr)\sin\psi\sin\beta$$

$$- (p^2 + q^2)\cos\beta] - \sin\zeta[-(\dot{q} + pr)\cos\psi\cos\beta - (\dot{p} - qr)\sin\psi\cos\beta$$

$$+ (p^2 + q^2)\sin\beta] + \cos\theta\cos\zeta[-(\dot{q} + pr)\sin\psi + (\dot{p} - qr)\cos\psi]\} + Q_{\zeta_2} \qquad (29)$$

$$\ddot{\beta}[\Delta e^2 m_\zeta + 2\Delta e M_\zeta\cos\zeta + I_\zeta(\cos^2\zeta + \sin^2\zeta\sin^2\theta)]$$

$$= \ddot{\zeta}\sin\theta(I_\zeta + \Delta e M_\zeta\cos\zeta) + (\ddot{\theta}\cos\theta\sin\zeta + 2\dot{\zeta}\dot{\theta}\cos\theta\cos\zeta - \dot{\theta}^2\sin\theta\sin\zeta)$$

$$\times (I_\zeta\cos\zeta + \Delta e M_\zeta) + (2\Omega\dot{\theta}\sin\theta\sin\zeta - 2\Omega\dot{\zeta}\cos\theta\cos\zeta - \dot{\Omega}\cos\theta\sin\zeta)$$

$$\times [I_\zeta(\sin\theta\cos\beta\sin\zeta - \sin\beta\cos\zeta) - \Delta e M_\zeta\sin\beta]$$

$$+ 2\dot{\beta}\dot{\zeta}\sin\zeta(I_\zeta\cos\zeta\cos^2\theta + \Delta e M_\zeta)$$

$$- 2\dot{\beta}\dot{\theta}I_\zeta\sin\theta\cos\theta\sin^2\zeta - \dot{\zeta}^2\Delta e M_\zeta\sin\theta\sin\zeta$$

$$+ \Omega^2\Big\{-\frac{1}{2}\sin 2\beta[\Delta e^2 m_\zeta + 2\Delta e M_\zeta\cos\zeta + I_\zeta(\cos^2\zeta - \sin^2\theta\sin^2\zeta)]$$

$$+ \frac{1}{2}I_\zeta\sin 2\zeta\cos 2\beta\sin\theta + \Delta e M_\zeta\sin\theta\sin\zeta\cos 2\beta$$

$$+ e_\beta M_\zeta(\cos\beta\sin\zeta\sin\theta - \sin\beta\cos\zeta) - \Delta e\, e_\beta m_\zeta\sin\beta\Big\}$$

$$- a_x\cos\psi[m_\zeta\Delta e\sin\beta - M_\zeta(\sin\theta\cos\beta\sin\zeta - \sin\beta\cos\zeta)]$$

$$- a_y\sin\psi[-m_\zeta\Delta e\sin\beta + M_\zeta(\sin\theta\cos\beta\sin\zeta - \sin\beta\cos\zeta)]$$

$$+ a_\zeta[-m_\zeta\Delta e\cos\beta + M_\zeta(\sin\theta\sin\beta\sin\zeta + \cos\beta\cos\zeta)]$$

$$- 2\dot{\zeta}\{-(q\sin\psi\sin\beta - p\cos\psi\sin\beta + r\cos\beta)I_\zeta\sin\theta\cos\theta\sin\zeta\cos\zeta$$

$$
\begin{aligned}
&+ (q \sin\psi \cos\beta - p \cos\psi \cos\beta)\cos\theta \cos\zeta(M_\zeta \Delta e - I_\zeta \cos\zeta) \\
&+ r \sin\beta \cos\theta \cos\zeta(M_\zeta \Delta e + I_\zeta \cos\zeta) + (q \cos\psi + p \sin\psi) \\
&\times [M_\zeta \Delta e \sin\zeta(1 - 2\cos^2\beta) + 2M_\zeta \Delta e \sin\beta \cos\beta \cos\zeta \sin\theta \\
&+ I_\zeta \sin\zeta \cos\zeta \cos^2\theta]\} \\
&- 2\dot{\theta}\{(q \sin\psi \sin\beta - p \cos\psi \sin\beta + r \cos\beta)I_\zeta \sin^2\theta \sin^2\zeta \\
&+ (q \sin\psi \cos\beta - p \cos\psi \cos\beta)\sin\theta \sin\zeta(-M_\zeta \Delta e + I_\zeta \cos\zeta) \\
&- r \sin\theta \sin\zeta \sin\beta(M_\zeta \Delta e + I_\zeta \cos\zeta) \\
&+ (q \cos\psi + p \sin\psi)\sin\zeta \cos\theta(2M_\zeta \Delta e \sin\beta \cos\beta - I_\zeta \sin\zeta \sin\theta)\} \\
&-2\dot{\beta}(q \cos\psi + p \sin\psi)[2M_\zeta \Delta e \sin\theta \sin\zeta \cos^2\beta \\
&- 2 \Delta e \sin\beta \cos\beta(M_\zeta \cos\zeta + m_\zeta \Delta e)] \\
&-2\Omega\{\sin\theta \sin\zeta(-p \cos\psi \sin\beta + q \sin\psi \sin\beta + r \cos\beta) \\
&\times [M_\zeta e_\beta + I_\zeta(\sin\beta \sin\zeta \sin\theta + \cos\beta \cos\zeta)] \\
&- \sin\theta \sin\zeta \cos\beta M_\zeta \Delta e(-p \cos\psi \sin\beta + q \sin\psi \sin\beta - r \cos\beta) \\
&- (p \cos\psi \cos\beta - q \sin\psi \cos\beta + r \sin\beta)[M_\zeta \cos\zeta(e_\beta + \Delta e \cos\beta) \\
&+ M_\zeta \Delta e \sin\beta \sin\theta \sin\zeta + I_\zeta \cos\zeta(\cos\beta \cos\zeta + \sin\beta \sin\zeta \sin\theta)] \\
&+ (p \cos\psi \cos\beta - q \sin\psi \cos\beta - r \sin\beta)[m_\zeta \Delta e(e_\beta + \Delta e \cos\beta) \\
&+ M_\zeta \Delta e \cos\beta \cos\zeta] - \cos\theta \sin\zeta(p \sin\psi + q \cos\psi) \\
&\times [-M_\zeta \Delta e \cos\beta + I_\zeta(\sin\theta \sin\zeta \sin\beta + \cos\zeta \cos\beta)]\} \\
&+ [(\dot{q} + pr)\cos\psi \sin\beta + (\dot{p} - qr)\sin\psi \sin\beta - (p^2 + q^2)\cos\beta] \\
&\times \{m_\zeta \Delta e(-\ell_z + \Delta e \sin\beta) - M_\zeta \Delta e(\cos\beta \sin\zeta \sin\theta - \cos\zeta \sin\beta)\} \\
&+ [(\dot{q} + pr)\cos\psi \sin\beta + (\dot{p} - qr)\sin\psi \sin\beta + (p^2 + q^2)\cos\beta] \\
&\times \{M_\zeta \cos\zeta(-\ell_z + \Delta e \sin\beta) + I_\zeta \cos\zeta(\cos\zeta \sin\beta - \sin\zeta \sin\theta \cos\beta)\} \\
&- [(\dot{q} + pr)\cos\psi \cos\beta + (\dot{p} - qr)\sin\psi \cos\beta - (p^2 + q^2)\sin\beta] \\
&\times \{M_\zeta \sin\theta \sin\zeta(-\ell_z + \Delta e \sin\beta)
\end{aligned}
$$

$$+ I_\zeta \sin\zeta \sin\theta(\sin\beta\cos\zeta - \cos\beta\sin\zeta\sin\theta)\}$$

$$- [(\dot{r} - qp)\cos\psi\sin\beta - (p^2 + r^2)\sin\psi\sin\beta - (\dot{p} + qr)\cos\beta]$$

$$\times \{M_\zeta \Delta e[\cos\psi\cos\theta\sin\zeta - \sin\psi(\cos\beta\cos\zeta + \sin\beta\sin\theta\sin\zeta)]$$

$$- m_\zeta \Delta e(e_\beta + \Delta e\cos\beta)\sin\psi\}$$

$$- [(\dot{r} - pq)\cos\psi\sin\beta - (p^2 + r^2)\sin\psi\sin\beta + (\dot{p} + qr)\cos\beta]$$

$$\times \{-\ell_y m_\zeta \Delta e - M_\zeta \cos\zeta[\ell_y + (e_\beta + \Delta e\cos\beta)\sin\psi]$$

$$+ I_\zeta \cos\zeta[\cos\psi\cos\theta\sin\zeta - \sin\psi(\cos\beta\cos\zeta + \sin\beta\sin\theta\sin\zeta)]\}$$

$$- [(\dot{r} - pq)\cos\psi\cos\beta - (p^2 + r^2)\sin\psi\cos\beta - (\dot{p} + qr)\sin\beta]$$

$$\times \{M_\zeta \sin\theta\sin\zeta[\ell_y + (e_\beta + \Delta e\cos\beta)\sin\psi] - I_\zeta \sin\zeta\sin\theta$$

$$\times [\cos\psi\cos\theta\sin\zeta - \sin\psi(\cos\beta\cos\zeta + \sin\beta\sin\theta\sin\zeta)]\}$$

$$+ [(q^2 + r^2)\cos\psi\sin\beta + (pq + \dot{r})\sin\psi\sin\beta + (\dot{q} - pr)\cos\beta]$$

$$\times \{m_\zeta \Delta e[\ell_x - (e_\beta + \Delta e\cos\beta)\cos\psi]$$

$$- M_\zeta \Delta e[\sin\psi\cos\theta\sin\zeta + \cos\psi(\cos\beta\cos\zeta + \sin\beta\sin\theta\sin\zeta)]\}$$

$$+ [(q^2 + r^2)\cos\psi\sin\beta + (pq + \dot{r})\sin\psi\sin\beta - (\dot{q} - pr)\cos\beta]$$

$$\times \{M_\zeta \cos\zeta[\ell_x - (e_\beta + \Delta e\cos\beta)\cos\psi] - I_\zeta \cos\zeta$$

$$\times [\sin\psi\cos\theta\sin\zeta + \cos\psi(\cos\beta\cos\zeta + \sin\beta\sin\theta\sin\zeta)]\}$$

$$+ [(q^2 + r^2)\cos\psi\cos\beta + (pq + \dot{r})\sin\psi\cos\beta + (\dot{q} - pr)\sin\beta]$$

$$\times \{-M_\zeta \sin\theta\sin\zeta[\ell_x - (e_\beta + \Delta e\cos\beta)\cos\psi] + I_\zeta \sin\theta\sin\zeta$$

$$\times [\sin\psi\cos\theta\sin\zeta + \cos\psi(\cos\beta\cos\zeta + \sin\beta\sin\theta\sin\zeta)]\} + Q_{\beta_2} \qquad (30)$$

In equations (29) and (30), m_ζ, M_ζ, and I_ζ are the zeroth, first, and second mass moments of the blade segment outboard of the lag hinge, i.e.,

$$m_\zeta = \int_o^R dm\ , \quad M_\zeta = \int_o^R r_\zeta\, dm\ , \quad I_\zeta = \int_o^R r_\zeta^2\, dm$$

The limits of integration for these quantities are from the lag hinge to the tip of the blade. When the effect of the inertia dynamics of the blade segment inboard of

the lag hinge is considered, additional terms as given by equation (A4) must be added to the right-hand side of the flapping equation (30) as discussed in detail in appendix A.

F-L-P Hinge Sequence

Now with the pitch bearing outboard of the lag hinge, the motion of the blade pitch no longer couples to the flap and lag motion. The coupled flap-lag equations of motion for the F-L-P hinge sequence can therefore be obtained directly from equations (29) and (30) by setting $\theta = \dot{\theta} = \ddot{\theta} = 0$. Alternatively, they can also be obtained using equations (20a), (20b), (21), (22), (25a), and (25b). The results are:

$$
\begin{aligned}
I_\zeta \ddot{\zeta} = {} & \dot{\Omega}[I_\zeta \cos\beta + M_\zeta \cos\zeta(e_\beta + \Delta e \cos\beta)] - 2\Omega\dot{\beta}\cos\zeta\sin\beta(I_\zeta\cos\zeta + \Delta e M_\zeta) \\
& - \dot{\beta}^2 \sin\zeta(I_\zeta\cos\zeta + \Delta e M_\zeta) + \Omega^2\left[\tfrac{1}{2} I_\zeta \sin^2\beta \sin 2\zeta\right. \\
& \left. - M_\zeta(e_\beta + \Delta e\cos\beta)\cos\beta\sin\zeta\right] + M_\zeta[a_x(\cos\zeta\sin\psi - \sin\zeta\cos\psi\cos\beta) \\
& + a_y(\cos\zeta\cos\psi + \sin\zeta\sin\psi\cos\beta) - a_z\sin\zeta\sin\beta] \\
& + 2\dot{\beta}(I_\zeta\cos\zeta + \Delta e M_\zeta)[\sin\zeta(q\cos\psi + p\sin\psi) \\
& - \cos\zeta(q\sin\psi\cos\beta - p\cos\psi\cos\beta - r\sin\beta)] \\
& + 2\Omega\{[M_\zeta(e_\beta + \Delta e\cos\beta) + I_\zeta\cos\beta\cos\zeta]\sin\zeta \\
& \times (q\sin\psi\sin\beta - p\cos\psi\sin\beta + r\cos\beta) \\
& - I_\zeta\sin\zeta[(q\cos\psi + p\sin\psi)\sin\zeta\sin\beta + r\cos\zeta]\} \\
& + \{M_\zeta[-\ell_x + (e_\beta + \Delta e\cos\beta)\cos\psi] + I_\zeta[\sin\psi\sin\zeta + \cos\psi\cos\beta\cos\zeta]\} \\
& \times \{-\sin\zeta[(q^2 + r^2)\cos\psi\cos\beta + (pq + \dot{r})\sin\psi\cos\beta + (\dot{q} - pr)\sin\beta] \\
& + \cos\zeta[(q^2 + r^2)\sin\psi - (pq + \dot{r})\cos\psi]\} \\
& + \{M_\zeta[\ell_y + (e_\beta + \Delta e\cos\beta)\sin\psi] - I_\zeta[\cos\psi\sin\zeta - \sin\psi\cos\beta\cos\zeta]\} \\
& \times \{-\sin\zeta[(pq - \dot{r})\cos\psi\cos\beta + (p^2 + r^2)\sin\psi\cos\beta + (\dot{p} + qr)\sin\beta] \\
& + \cos\zeta[(pq - \dot{r})\sin\psi - (p^2 + r^2)\cos\psi]\} \\
& + \{M_\zeta(-\ell_z + \Delta e\sin\beta) + I_\zeta\sin\beta\cos\zeta\}
\end{aligned}
$$

$$\times \{-\sin\zeta[-(\dot{q} + pr)\cos\psi\cos\beta - (\dot{p} - qr)\sin\psi\cos\beta + (p^2 + q^2)\sin\beta]$$

$$+ \cos\zeta[-(\dot{q} + pr)\sin\psi + (\dot{p} - qr)\cos\psi]\} + Q_{\zeta_3} \tag{31}$$

$$\ddot{\beta}[\Delta e^2 m_\zeta + 2\,\Delta e M_\zeta \cos\zeta + I_\zeta \cos^2\zeta]$$

$$= (2\Omega\dot{\zeta}\cos\zeta + \dot{\Omega}\sin\zeta)(I_\zeta\cos\zeta + \Delta e M_\zeta)\sin\beta + 2\dot{\beta}\dot{\zeta}\sin\zeta(I_\zeta\cos\zeta + \Delta e M_\zeta)$$

$$+ \Omega^2\left\{-\frac{1}{2}(\Delta e^2 m_\zeta + 2\,\Delta e M_\zeta\cos\zeta + I_\zeta\cos^2\zeta)\sin 2\beta\right.$$

$$\left. - e_\beta\sin\beta(M_\zeta\cos\zeta + \Delta e m_\zeta)\right\} - \sin\beta(M_\zeta\cos\zeta + \Delta e m_\zeta)(a_x\cos\psi - a_y\sin\psi)$$

$$+ \cos\beta(M_\zeta\cos\zeta - \Delta e m_\zeta)a_z - 2\dot{\zeta}\{\cos\zeta[\cos\beta(q\sin\psi - p\cos\psi)$$

$$\times (M_\zeta\,\Delta e - I_\zeta\cos\zeta) + r\sin\beta(M_\zeta\,\Delta e + I_\zeta\cos\zeta)]$$

$$+ \sin\zeta(q\cos\psi + p\sin\psi)[M_\zeta\,\Delta e(1 - 2\cos^2\beta) + I_\zeta\cos\zeta]\}$$

$$+ 2\dot{\beta}(q\cos\psi + p\sin\psi)(M_\zeta\cos\zeta + m_\zeta\,\Delta e)\Delta e\sin 2\beta$$

$$+ 2\Omega\{\cos\zeta(p\cos\psi\cos\beta - q\sin\psi\cos\beta + r\sin\beta)$$

$$\times [M_\zeta(e_\beta + \Delta e\cos\beta) + I_\zeta\cos\beta\cos\zeta] + \sin\zeta(p\sin\psi + q\cos\psi)$$

$$\times [-M_\zeta\,\Delta e\cos\beta + I_\zeta\cos\zeta\cos\beta]$$

$$- (p\cos\psi\cos\beta - q\sin\psi\cos\beta - r\sin\beta)$$

$$\times [m_\zeta\,\Delta e(e_\beta + \Delta e\cos\beta) + M_\zeta\,\Delta e\cos\beta\cos\zeta]\}$$

$$+ [(\dot{q} + pr)\cos\psi\sin\beta + (\dot{p} - qr)\sin\psi\sin\beta - (p^2 + q^2)\cos\beta]\Delta e$$

$$\times [m_\zeta(-\ell_z + \Delta e\sin\beta) + M_\zeta\cos\zeta\sin\beta]$$

$$+ [(\dot{q} + pr)\cos\psi\sin\beta + (\dot{p} - qr)\sin\psi\sin\beta + (p^2 + q^2)\cos\beta]\cos\zeta$$

$$\times [M_\zeta(-\ell_z + \Delta e\sin\beta) + I_\zeta\cos\zeta\sin\beta]$$

$$- [(\dot{r} - qp)\cos\psi\sin\beta - (p^2 + r^2)\sin\psi\sin\beta - (\dot{p} + qr)\cos\beta]\Delta e$$

$$\times [M_\zeta(\cos\psi\sin\zeta - \sin\psi\cos\beta\cos\zeta) - m_\zeta(e_\beta + \Delta e\cos\beta)\sin\psi]$$

$$- [(\dot{r} - qp)\cos\psi\sin\beta - (p^2 + r^2)\sin\psi\sin\beta + (\dot{p} + qr)\cos\beta]$$

$$\times \{-\ell_y m_\zeta\,\Delta e - M_\zeta\cos\zeta[\ell_y + (e_\beta + \Delta e\cos\beta)\sin\psi]$$

$$+ I_\zeta\cos\zeta[\cos\psi\sin\zeta - \sin\psi\cos\beta\cos\zeta]\}$$

$$+ [(q^2 + r^2)\cos\psi \sin\beta + (pq + \dot{r})\sin\psi \sin\beta + (\dot{q} - pr)\cos\beta]\Delta e$$

$$\times \{m_\zeta[\ell_x - (e_\beta + \Delta e \cos\beta)\cos\psi] - M_\zeta[\sin\psi \sin\zeta + \cos\psi \cos\beta \cos\zeta]\}$$

$$+ [(q^2 + r^2)\cos\psi \sin\beta + (pq + \dot{r})\sin\psi \sin\beta - (\dot{q} - pr)\cos\beta]\cos\zeta$$

$$\times \{M_\zeta[\ell_x - (e_\beta + \Delta e \cos\beta)\cos\psi] - I_\zeta[\sin\psi \sin\zeta + \cos\psi \cos\beta \cos\zeta]\}$$

$$+ Q_{\beta_3} \tag{32}$$

Equation (31) provides the complete inertia dynamics for the lead-lag equation of motion. However, as with the F-P-L hinge sequence, additional terms, as given by equation (A4), must be included in the right-hand side of the flapping equation (32), when the effect of the inertia dynamics associated with the blade segment inboard of the lag hinge is considered.

COMPARISON OF THE RESULTS WITH PREVIOUS WORK

The inertia dynamics in the coupled flap-lag equations of motion for the three hinge sequences, as shown in equations (26) through (32), are now compared with available results in the literature. In general, the previous results have tended to be only for one specific hinge sequence or with limited considerations for the effects of aircraft motions.

L-F-P Hinge Sequence

A complete derivation of the inertia dynamics for the coupled flap-lag equations of motion, including some effects of aircraft motions, is given in reference 11 for an L-F-P hinge sequence with co-located flap and lag hinges. Reference 3 also provides an approximation for the same configuration. This specific hub configuration can be obtained by setting $\Delta e = 0$ in equations (26) and (27) to yield:

$$\ddot{\zeta} = \frac{M_\beta}{I_\beta \cos\beta}\{a_x \sin(\psi - \zeta) + a_y \cos(\psi - \zeta)$$

$$+ e_\zeta[(\dot{\Omega} - \dot{r})\cos\zeta - (\Omega - r)^2 \sin\zeta - pq\cos(2\psi - \zeta)$$

$$- p^2 \sin\psi \cos(\psi - \zeta) + q^2 \cos\psi \sin(\psi - \zeta)]$$

$$+ \ell_x[(\dot{r} + qp)\cos(\psi - \zeta) - (q^2 + r^2)\sin(\psi - \zeta)]$$

$$+ \ell_y[(pq - \dot{r})\sin(\psi - \zeta) - (p^2 + r^2)\cos(\psi - \zeta)]$$

$$- \underline{\ell_z}[(\dot{p} - qr)\cos(\psi - \zeta) - (\dot{q} + pr)\sin(\psi - \zeta)]\}$$

$$+ \tan\beta[2\dot{\beta}(r - \Omega + \dot{\zeta}) + (\dot{p} - qr)\cos(\psi - \zeta) - (\dot{q} + pr)\sin(\psi - \zeta)]$$

$$+ (\dot{\Omega} - \dot{r}) + 2\dot{\beta}[p\cos(\psi - \zeta) - q\sin(\psi - \zeta)] - pq\cos 2(\psi - \zeta)$$

$$- \frac{1}{2}(p^2 - q^2)\sin 2(\psi - \zeta) + \frac{Q_{\zeta_1}}{I_\beta \cos^2\beta} \tag{33}$$

and

$$\ddot{\beta} = \frac{M_\beta}{I_\beta}\{\sin\beta\{-a_x\cos(\psi - \zeta) + a_y\sin(\psi - \zeta) - e_\zeta[\dot{\Omega}\sin\zeta + (\Omega^2 - 2r\Omega)\cos\zeta]$$

$$+ (\underline{\ell_x} - e_\zeta\cos\psi)[(\dot{r} + pq)\sin(\psi - \zeta) + (q^2 + r^2)\cos(\psi - \zeta)]$$

$$+ (\underline{\ell_y} + e_\zeta\sin\psi)[(\dot{r} - pq)\cos(\psi - \zeta) - (p^2 + r^2)\sin(\psi - \zeta)]$$

$$- \underline{\ell_z}[(\dot{p} - qr)\sin(\psi - \zeta) + (\dot{q} + pr)\cos(\psi - \zeta)]\}$$

$$+ \cos\beta\{a_z + 2\Omega e_\zeta(p\cos\psi - q\sin\psi) - (\dot{q} - pr)(\underline{\ell_x} - e_\zeta\cos\psi)$$

$$+ (\dot{p} + qr)(\underline{\ell_y} + e_\zeta\sin\psi) - (p^2 + q^2)\underline{\ell_z}\}\}$$

$$+ \sin\beta\{[(\dot{p} - qr)\sin(\psi - \zeta) + (\dot{q} + pr)\cos(\psi - \zeta)]\sin\beta$$

$$- \{[p\sin(\psi - \zeta) + q\cos(\psi - \zeta)]^2 + [r - (\Omega - \dot{\zeta})]^2\}\cos\beta\}$$

$$+ \cos\beta\{(p^2 + q^2)\sin\beta + \{2(\Omega - \dot{\zeta})[p\cos(\psi - \zeta) - q\sin(\psi - \zeta)]$$

$$+ (\dot{p} + qr)\sin(\psi - \zeta) + (\dot{q} - pr)\cos(\psi - \zeta)\}\cos\beta\} + \frac{Q_{\beta_1}}{I_\beta} \tag{34}$$

Note that the underlined quantities in equations (33) and (34) are not included in reference 11 because the effects of the displacement between the hub center and the aircraft c.g. have not been considered. These effects are considered in the present development, allowing applications to tandem or side-by-side dual-rotor configurations where the offset between the hub center and aircraft c.g. are generally large and therefore cannot be neglected. Note also that the sign convention used in this report for the lead-lag angle is positive for lagging (roughly, measured positive when opposite to the direction of rotor rotation). Several other reports (e.g., refs. 3, 5, 9, and 11) use different sign convention.

F-P-L Hinge Sequence

A comprehensive flap-lag rotor analysis was reported in reference 10 for the F-P-L hinge sequence for tandem-rotor applications. The present work expands the effects due to aircraft motion to account for lateral offset ℓ_y which is necessary for modeling tilt-rotor or side-by-side dual-rotor configurations. The inertia moment for the blade segment inboard of the lag hinge, which was neglected in reference 10, is also included in the present work for completeness (appendix A).

F-L-P Hinge Sequence

This hinge sequence (as well as the L-F-P hinge sequence) was considered in reference 9 for centrally co-located flap and lag hinges; no hinge offsets were included. Nor were the effects of aircraft motions considered in that work. Reference 5 provides a list of the inertia dynamic terms for this hinge sequence. Unfortunately, neither the effects of the variation in the angular velocity of the rotor system nor the effects of aircraft motion were included. As discussed earlier, the effects of aircraft motions, which need to be considered for flight dynamics and control applications, drastically complicates the coupled flap-lag equations of motion as evident from equations (31) and (32). When these effects are neglected, equations (31), (32), and (A4) in appendix A reduce to simply

$$I_\zeta \ddot{\zeta} = \underline{\dot{\Omega}[I_\zeta \cos\beta + M_\zeta(e_\beta + \Delta e \cos\beta)\cos\zeta]} - 2\Omega\dot{\beta}\sin\beta\cos\zeta(I_\zeta\cos\zeta + \Delta eM_\zeta) - \dot{\beta}^2\sin\zeta(I_\zeta\cos\zeta + \Delta eM_\zeta) + \Omega^2 \times \left[\frac{1}{2} I_\zeta \sin^2\beta \sin 2\zeta - M_\zeta(e_\beta + \Delta e\cos\beta)\cos\beta\sin\zeta\right] + Q_{\zeta_3} \tag{35}$$

$$[\Delta e^2 m_\zeta + 2\Delta eM_\zeta\cos\zeta + I_\zeta\cos^2\zeta + I_{\Delta e}]\ddot{\beta} = (2\Omega\dot{\zeta}\cos\zeta + \underline{\dot{\Omega}\sin\zeta})(I_\zeta\cos\zeta + \Delta eM_\zeta)\sin\beta + 2\dot{\beta}\dot{\zeta}\sin\zeta(I_\zeta\cos\zeta + \Delta eM_\zeta) - \Omega^2\left[\frac{1}{2}(\Delta e^2 m_\zeta + 2\Delta eM_\zeta\cos\zeta + I_\zeta\cos^2\zeta)\sin 2\beta + e_\beta\sin\beta(M_\zeta\cos\zeta + \Delta em_\zeta) + (I_{\Delta e}\cos\beta + e_\beta M_{\Delta e})\sin\beta\right] + Q_{\beta_3} \tag{36}$$

When the effects of the variation in rotor rpm, as indicated by the underlined terms in equations (35) and (36), are neglected, these equations reduce to those shown in reference 5.

We now turn to examine two special cases: (1) co-located hinges with another hinge sequence, F-L-P, and (2) elimination of the lead-lag degree of freedom.

When the flapping and lag hinges are co-located, the inertia dynamics for the coupled flap-lag equations can also be readily obtained by simply setting $\Delta e = 0$ in equations (31) and (32). It is important to note, however, that the resulting

expressions will be different from equations (33) and (34) for the L-F-P hinge sequence, because the sequence of rotation associated with flapping and lag angles is different, thereby resulting in a different definition associated with these two angles (similar to the situation when the sequence of rotation is changed, the definition of Euler angles must change accordingly). It is for this reason that equations (26) and (27) were used as the basis for equations (33) and (34).

Finally, in the absence of the lead-lag degree of freedom, it can be seen from equations (26) through (32) that the inertia dynamics for all three hinge sequences collapse to the same identical flapping dynamics as shown in equation (37).

$$
\begin{aligned}
I_\beta \ddot{\beta} = {} & -\Omega^2\left(eM_\beta \sin\beta + \frac{1}{2} I_\beta \sin 2\beta\right) - [(a_x \cos\psi - a_y \sin\psi)\sin\beta - a_z \cos\beta]M_\beta \\
& + 2\Omega(p\cos\psi\cos\beta - q\sin\psi\cos\beta + r\sin\beta)(M_\beta e_\beta + I_\beta \cos\beta) \\
& + [(\dot{q} + pr)\cos\psi\sin\beta + (\dot{p} - qr)\sin\psi\sin\beta + (p^2 + q^2)\cos\beta] \\
& \times (-M_\beta \ell_z + I_\beta \sin\beta) + [(\dot{r} - pq)\cos\psi\sin\beta - (p^2 + r^2)\sin\psi\sin\beta \\
& + (\dot{p} + qr)\cos\beta][M_\beta(\ell_y + e_\beta \sin\psi) + I_\beta \sin\psi\cos\beta] \\
& + [(q^2 + r^2)\cos\psi\sin\beta + (pq + \dot{r})\sin\psi\sin\beta - (\dot{q} - pr)\cos\beta] \\
& \times [M_\beta(\ell_x - e_\beta \cos\psi) - I_\beta \cos\psi\cos\beta] + Q_\beta
\end{aligned}
\tag{37}
$$

Equation (37) represents an extension of reference 14 by including all the flapping effects due to aircraft motion.

DETERMINATION OF THE GENERALIZED FORCES

The generalized forces (refs. 22 and 23) associated with the flapping and lead-lag motions, which are symbolically shown on the right-hand side of equations (26) through (32), consist of contributions from the gravitational force, aerodynamic forces, and the forces due to lag dampers and hinge springs. Determination of those contributions requires first calculating the virtual work of an individual contributing external force associated with the virtual flapping and lead-lag displacements. Let X_i, Y_i, Z_i be the components of the ith external force F_i acting on the blade element dr when expressed in the hub-body x,y,z frame of reference. Then the resulting elemental virtual work done by this external force due to the virtual flapping and lag displacements $\delta\beta$ and $\delta\zeta$ is

$$
\delta W_i = X_i \delta x + Y_i \delta y + Z_i \delta z \tag{38a}
$$

where

$$\delta x = \frac{\partial x}{\partial \beta}\,\delta\beta + \frac{\partial x}{\partial \zeta}\,\delta\zeta$$

$$\delta y = \frac{\partial y}{\partial \beta}\,\delta\beta + \frac{\partial y}{\partial \zeta}\,\delta\zeta \tag{38b}$$

$$\delta z = \frac{\partial z}{\partial \beta}\,\delta\beta + \frac{\partial z}{\partial \zeta}\,\delta\zeta$$

and x,y,z are the coordinates of the blade element as given by equations (2), (14), and (19) for the three hinge sequences being considered. Now, summing up the elemental virtual work over the appropriate blade span results in the total virtual work δW_t

$$\delta W_t = \int\left(X_i \frac{\partial x}{\partial \beta} + Y_i \frac{\partial y}{\partial \beta} + Z_i \frac{\partial z}{\partial \beta}\right)\delta\beta + \int\left(X_i \frac{\partial x}{\partial \zeta} + Y_i \frac{\partial y}{\partial \zeta} + Z_i \frac{\partial z}{\partial \zeta}\right)\delta\zeta \tag{39a}$$

By equating the total virtual work δW_t to the virtual work of the generalized forces along the virtual displacement in the generalized coordinates, i.e., $\delta W_t = Q_\beta \delta\beta + Q_\zeta \delta\zeta$, the generalized forces associated with that external force F_i are determined:

$$Q_{\beta,i} = \int\left(X_i \frac{\partial x}{\partial \beta} + Y_i \frac{\partial y}{\partial \beta} + Z_i \frac{\partial z}{\partial \beta}\right) \tag{39b}$$

$$Q_{\zeta,i} = \int\left(X_i \frac{\partial x}{\partial \zeta} + Y_i \frac{\partial y}{\partial \zeta} + Z_i \frac{\partial z}{\partial \zeta}\right) \tag{39c}$$

As an example, the generalized forces Q_{ζ_3} and Q_{β_3} in equations (31) and (32) for the F-L-P hinge sequence will be derived in detail below to illustrate the procedure. Let

$$Q_{\zeta_3} = Q_{\zeta,G} + Q_{\zeta,A} + Q_{\zeta,D} + Q_{\zeta,S} \tag{40a}$$

$$Q_{\beta_3} = Q_{\beta,G} + Q_{\beta,A} + Q_{\beta,D} + Q_{\beta,S} \tag{40b}$$

representing the contributions from the gravity force, aerodynamic forces, and the forces due to dampers and hinge springs. We will consider each of these forces separately.

Gravity Force Contribution, $Q_{\zeta,G}$ and $Q_{\beta,G}$

The gravity force acting on a blade element with mass dm can be expressed in the hub-body system of reference using a sequence of transformation, equations (4b) and (4a), from inertia to aircraft body to hub-body systems. The result is

$$\begin{aligned} X_G &= g\,dm\,A_1 \\ Y_G &= g\,dm\,A_2 \\ Z_G &= g\,dm\,A_3 \end{aligned} \tag{41}$$

where

$$\begin{aligned} A_1 &= \sin i \cos \phi_a \cos \theta_a - \cos i \sin \theta_a \\ A_2 &= \sin \phi_a \cos \theta_a \\ A_3 &= \cos i \cos \phi_a \cos \theta_a + \sin i \sin \theta_a \end{aligned} \tag{42}$$

From equation (19), the virtual displacement, in the hub-body system, of the blade element outboard of the lag hinge is obtained.

$$\begin{aligned} \delta x &= (\Delta e \sin \beta + r_\zeta \sin \beta \cos \zeta)\cos \psi \delta\beta + r_\zeta(\cos \beta \sin \zeta \cos \psi - \cos \zeta \sin \psi)\delta\zeta \\ \delta y &= -(\Delta e \sin \beta + r_\zeta \sin \beta \cos \zeta)\sin \psi \delta\beta - r_\zeta(\cos \beta \sin \zeta \sin \psi + \cos \zeta \cos \psi)\delta\zeta \\ \delta z &= -(\Delta e + r_\zeta \cos \zeta)\cos \beta \delta\beta + r_\zeta \sin \zeta \sin \beta \delta\zeta \end{aligned} \tag{43}$$

The coordinates for a blade element between the two hinges, measured r_β from the flapping hinge, are

$$\begin{aligned} x &= -(e_\beta + r_\beta \cos \beta)\cos \psi \\ y &= (e_\beta + r_\beta \cos \beta)\sin \psi \\ z &= -r_\beta \sin \beta \end{aligned} \tag{44}$$

and therefore,

$$\delta x = r_\beta \sin\beta \cos\psi \delta\beta$$

$$\delta y = -r_\beta \sin\beta \sin\psi \delta\beta \tag{45}$$

$$\delta z = -r_\beta \cos\beta \delta\beta$$

which are independent of the virtual displacement in the lead-lag motion.

Substituting equations (41)-(43) and (45) into equation (39), the desired generalized forces due to gravity are obtained.

$$Q_{\zeta,G} = -gM_\zeta[(A_1 \sin\psi + A_2 \cos\psi)\cos\zeta + (A_2 \sin\psi - A_1 \cos\psi)\cos\beta \sin\zeta - A_3 \sin\beta \sin\zeta] \tag{46}$$

$$Q_{\beta,G} = g(\Delta em_\zeta + M_\zeta \cos\zeta + M_{\Delta e})[(A_1 \cos\psi - A_2 \sin\psi)\sin\beta - A_3 \cos\beta] \tag{47}$$

Equations (46) and (47) represent a generalization of the results given previously in references 5 and 10 by including in Q_{β_3} both the effects of shaft tilt angle and the weight moment inboard of the lag hinge. Note that equations (46) and (47) can alternatively be obtained using appropriate coordinate transformations listed in appendix B, and by considering the blade weight moment about the lag and flapping hinges as were done in references 5 and 10.

Aerodynamic Force Contribution, $Q_{\beta,A}$ and $Q_{\zeta,A}$

The elementary aerodynamic forces acting on the blade element, dL and dD, are resolved first in the plane perpendicular to the blade span in a manner as illustrated in figures 7(a) and 7(b).

$$dD_1 = dD \cos\phi_r - dL \sin\phi_r \tag{48a}$$

$$dL_1 = dL \cos\phi_r + dD \sin\phi_r \tag{48b}$$

where

$$dD = 1/2\ \rho U^2 c_d c\ dr_\zeta \tag{49a}$$

$$dL = 1/2\ \rho U^2 c_\ell c\ dr_\zeta \tag{49b}$$

$$U^2 = u_T^2 + u_P^2 \tag{49c}$$

$$\phi_r = \tan^{-1}(u_P/u_T) \tag{49d}$$

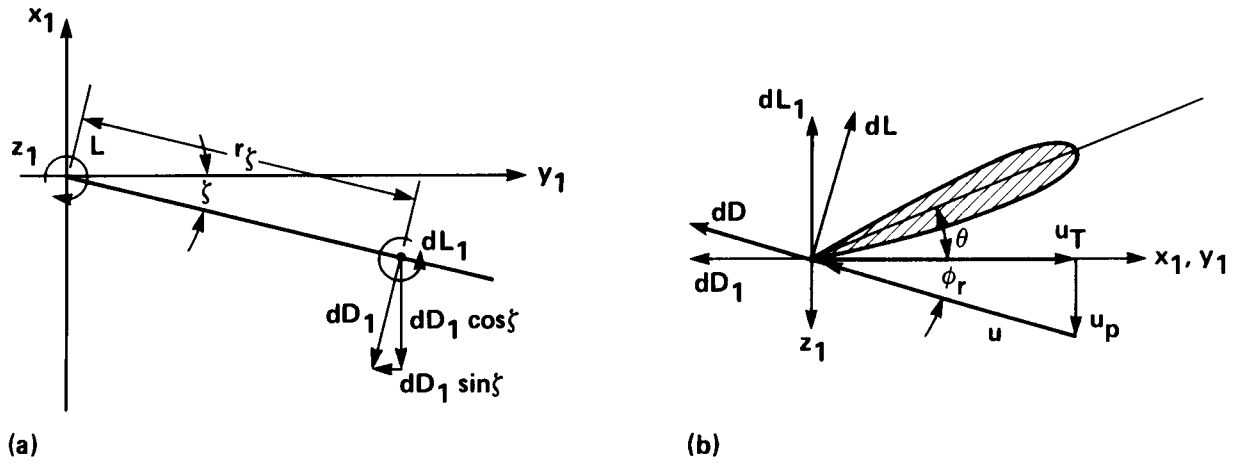

Figure 7.- Elemental aerodynamic forces. (a) Force diagram in x_1-y_1 plane; (b) resolution of elementary lift and drag forces.

Note that the section lift and drag coefficients c_ℓ and c_d in equations (49a) and (49b) are functions of the local angle of attack α_r and Mach number M_r (ref. 24).[1] The calculation of α_r and the airspeed components u_p and u_T will be discussed later.

When expressed in the x_1,y_1,z_1 frame of reference, the components of the aerodynamic force are

$$\begin{Bmatrix} X_1 \\ Y_1 \\ Z_1 \end{Bmatrix}_A = \begin{Bmatrix} -dD_1 \cos\zeta \\ -dD_1 \sin\zeta \\ -dL_1 \end{Bmatrix} \tag{50}$$

From equations (B7) and (B8), these components can be transformed into those in the hub-body system

$$\begin{Bmatrix} X_A \\ Y_A \\ Z_A \end{Bmatrix} = \begin{Bmatrix} -dD_1(\cos\zeta \sin\psi - \sin\zeta \cos\beta \cos\psi) + dL_1 \sin\beta \cos\psi \\ -dD_1(\cos\zeta \cos\psi + \sin\zeta \cos\beta \sin\psi) - dL_1 \sin\beta \sin\psi \\ dD_1 \sin\zeta \sin\beta - dL_1 \cos\beta \end{Bmatrix} \tag{51}$$

Using equations (51), (43), (39b), and (39c), the aerodynamic force contributions to the generalized forces in equations (40a) and (40b) are obtained.

[1]Extensions of the two-dimensional airfoil data may be made to include the spanwise flow effect (refs. 25 and 26), unsteady effects (refs. 26-29), and dynamic inflow (ref. 30).

$$Q_{\beta,A} = \int_{r_c}^{R} \frac{1}{2} \rho U^2 c_d c \sin \phi_r (\Delta e + r_\zeta \cos \zeta) dr_\zeta$$

$$+ \int_{r_c}^{BR} \frac{1}{2} \rho U^2 c_\ell c \cos \phi_r (\Delta e + r_\zeta \cos \zeta) dr_\zeta \tag{52}$$

$$Q_{\zeta,A} = \int_{r_c}^{R} \frac{1}{2} \rho U^2 c_d c \cos \phi_r r_\zeta \, dr_\zeta$$

$$- \int_{r_c}^{BR} \frac{1}{2} \rho U^2 c_\ell c \sin \phi_r r_\zeta \, dr_\zeta \tag{53}$$

Note that in setting up the limits of integration in equations (52) and (53), the blade cutoff is assumed to extend beyond the blade segment outboard of the lag hinge. Note also that in calculating the total blade lift, a tip loss factor B is used, thereby effectively limiting the lift of the blade beyond BR.

The calculation of the components of the velocity (with respect to the air mass), u_P and u_T, and the local angle of attack, α_r, is now addressed. The velocity of the blade element due to blade and aircraft motions has been obtained previously as shown in equation (20). Additional contributions to the total local airspeed components in the hub-body system are due to rotor-induced velocity and wind and turbulence. The resultant airspeed components in the hub-body system are then transformed into x_1, y_1, z_1 frame of reference using equation (B9). Let the resultant local airspeed components be denoted by $\dot{x}_1, \dot{y}_1, \dot{z}_1$. Then, u_P, u_T, and u_S (the spanwise component) are given by

$$u_P = \dot{z}_1 \tag{54a}$$

$$u_T = \dot{x}_1 \cos \zeta + \dot{y}_1 \sin \zeta \tag{54b}$$

$$u_S = -\dot{x}_1 \sin \zeta + \dot{y}_1 \cos \zeta \tag{54c}$$

The local angle of attack of the blade element consists of ϕ_r and the blade pitch setting, which includes, for generality, collective and cyclic pitch, blade twist, and pitch-flap and pitch-lag couplings, K_1 and K_2, as shown in equation (55).

$$\alpha_r = \phi_r + \theta_o - A_{1s} \cos \psi - B_{1s} \sin \psi + \theta_{t,r} - K_1 \beta - K_2 \zeta \tag{55}$$

This concludes the formulation of quantities that are necessary to compute the aerodynamic contribution to the generalized forces.

Contributions from Spring Restraints and Dampers

The generalized forces corresponding to the spring restraints and dampers can be obtained directly (ref. 23) from the potential energy for the hub springs, $(1/2)K_\beta\beta^2 + (1/2)K_\zeta\zeta^2$, and the dissipation functions for the dampers, $(1/2)C_\beta\dot{\beta}^2 + (1/2)C_\zeta\dot{\zeta}^2$, respectively. For generality, a provision is made, permitting either the representation of the actual springs/viscous dampers or the simulation of the structural stiffness/damping. These generalized forces are:

$$Q_{\zeta,S} = -K_\zeta\zeta \tag{56a}$$

$$Q_{\beta,S} = -K_\beta\beta \tag{56b}$$

$$Q_{\zeta,D} = -C_\zeta\dot{\zeta} \tag{56c}$$

$$Q_{\beta,D} = -C_\beta\dot{\beta} \tag{56d}$$

This concludes the development of all the factors contributing to the generalized forces in equations (40a) and (40b) for the F-L-P hinge sequence. The generalized forces for the other two hinge sequences considered can be developed in a similar fashion. Results are shown in appendix C.

CONCLUDING REMARKS

Flap-lag equations of motion for a rigid articulated rotor blade have been developed for three widely used flap, lag, and pitch hinge sequences. The effects of the complete six degrees-of-freedom of aircraft motions were included and all the inertia dynamic terms were retained. Comparisons of the results of this development, which uses the Lagrangian method, with those available in the literature were made to identify, with special emphasis on the inertia dynamics, the source of terms missing in previous analyses.

This effort represents the first step toward developing a generic blade-element rotor model suitable for full-flight envelope, real-time, flight dynamic simulation of various rotorcraft. Subsequent steps will involve the development of detailed equations for the calculation of the rotor forces and moments, and the development of appropriate approximate models for specific applications. To permit comparisons with flexible blade analysis planned for a later date, a provision is made in the present analysis to allow for representation of the actual hub springs and viscous dampers or simulation of the structural stiffness and damping in both the flapping and lead-lag degrees of freedom. In addition, kinematic feedback couplings in pitch-flap and pitch-lag have also been included.

APPENDIX A

INERTIA DYNAMICS OF THE BLADE SEGMENT BETWEEN THE FLAPPING AND LAG HINGES

In the development of the coupled flap-lag equations of motion, the inertia dynamics associated with the blade segment between the flapping and lag hinges were neglected. For completeness, additional terms due to this blade segment are developed here for the three hinge sequences considered.

L-F-P Hinge Sequence

For this hinge sequence, the portion of the rotor blade inboard of the flapping hinge involves only the lead-lag motion. As a result, the inertia dynamics associated with this segment contribute only to the lead-lag equation of motion (26); however, they have no effects on the flapping equation of motion (27).

The total velocity of a blade element between the flapping and lag hinges, a distance r_ζ from the lag hinge, can readily be obtained from equations (6) and (7) by setting $\beta = \dot{\beta} = 0$, $r_\beta = 0$, and by replacing Δe with r_ζ. The results are:

$$V_r = \begin{Bmatrix} \dot{x} + \Delta\dot{x} \\ \dot{y} + \Delta\dot{y} \\ \dot{z} + \Delta\dot{z} \end{Bmatrix} \tag{A1a}$$

where

$$\begin{aligned} \dot{x} &= e_\zeta \Omega \sin\psi + r_\zeta(\Omega - \dot{\zeta})\sin(\psi - \zeta) \\ \dot{y} &= e_\zeta \Omega \cos\psi + r_\zeta(\Omega - \dot{\zeta})\cos(\psi - \zeta) \\ \dot{z} &= 0 \end{aligned} \tag{A1b}$$

and

$$\begin{aligned} \Delta\dot{x} &= \dot{x}_o + q\ell_z - r[(\ell_y + e_\zeta \sin\psi) + r_\zeta \sin(\psi - \zeta)] \\ \Delta\dot{y} &= \dot{y}_o - p\ell_z + r[(\ell_x - e_\zeta \cos\psi) - r_\zeta \cos(\psi - \zeta)] \\ \Delta\dot{z} &= \dot{z}_o + p[(\ell_y + e_\zeta \sin\psi) + r_\zeta \sin(\psi - \zeta)] \\ &\quad - q[(\ell_x - e_\zeta \cos\psi) - r_\zeta \cos(\psi - \zeta)] \end{aligned} \tag{A1c}$$

Using equations (21) through (25a), the inertia dynamics associated with the blade segment can be obtained as shown in equation (A2). These additional terms are to be added to the right-hand side of equation (26) to provide the complete set of inertia dynamics for the single rotor blade. Note that equation (A2) can also be directly obtained from equation (33) by setting $\beta = \dot{\beta} = 0$ and by replacing M_β and I_β with $M_{\Delta e}$ and $I_{\Delta e}$, respectively.

$$
\begin{aligned}
&-I_{\Delta e}\ddot{\zeta} + I_{\Delta e}\left[(\dot{\Omega} - \dot{r}) - \frac{1}{2}(p^2 - q^2)\sin 2(\psi - \zeta) - pq\cos 2(\psi - \zeta)\right] \\
&\quad + M_{\Delta e}\{a_x \sin(\psi - \zeta) + a_y \cos(\psi - \zeta) + e_\zeta[(\dot{\Omega} - \dot{r})\cos\zeta - (\Omega - r)^2 \sin\zeta \\
&\quad - pq\cos(2\psi - \zeta) - p^2 \sin\psi\cos(\psi - \zeta) + q^2 \cos\psi \sin(\psi - \zeta)] \\
&\quad + \ell_x[(\dot{r} + pq)\cos(\psi - \zeta) - (q^2 + r^2)\sin(\psi - \zeta)] \\
&\quad + \ell_y[(pq - \dot{r})\sin(\psi - \zeta) - (p^2 + r^2)\cos(\psi - \zeta)] \\
&\quad - \ell_z[(\dot{p} - qr)\cos(\psi - \zeta) - (\dot{q} + pr)\sin(\psi - \zeta)]\}
\end{aligned}
\tag{A2}
$$

where

$$M_{\Delta e} = \int_o^{\Delta e} r_\zeta \, dm$$

$$I_{\Delta e} = \int_o^{\Delta e} r_\zeta^2 \, dm$$

F-P-L and F-L-P Hinge Sequences

The effect of the inertia dynamics of the blade segment inboard of the lag hinge on the flapping equation of motion is identical for the F-P-L and the F-L-P hinge sequences. This blade segment involves only flapping motion and therefore its inertia dynamics have no effects on the lead-lag equation of motion, equation (29) or (31).

The total velocity of a blade element between the flapping and lag hinges, measured r_β from the flapping hinge, can be obtained from equations (20a) and (20b) by setting $\zeta = \dot{\zeta} = 0$ and by replacing Δe with r_β to yield equations (A1a), (A3a), and (A3b).

$$
\begin{aligned}
\dot{x} &= (e_\beta + r_\beta \cos\beta)\Omega \sin\psi + r_\beta\dot{\beta}\cos\psi\sin\beta \\
\dot{y} &= (e_\beta + r_\beta \cos\beta)\Omega \cos\psi - r_\beta\dot{\beta}\sin\psi\sin\beta \\
\dot{z} &= -r_\beta\dot{\beta}\cos\beta
\end{aligned}
\tag{A3a}
$$

$$\Delta\dot{x} = \dot{x}_o + q(\ell_z - r_\beta \sin\beta) - r[\ell_y + (e_\beta + r_\beta \cos\beta)\sin\psi]$$

$$\Delta\dot{y} = \dot{y}_o + r[\ell_x - (e_\beta + r_\beta \cos\beta)\cos\psi] - p(\ell_z - r_\beta \sin\beta) \qquad \text{(A3b)}$$

$$\Delta\dot{z} = \dot{z}_o - q[\ell_x - (e_\beta + r_\beta \cos\beta)\cos\psi] + p[\ell_y + (e_\beta + r_\beta \cos\beta)\sin\psi]$$

Using equations (21) through (24) and (25b), the inertia dynamics associated with the blade segment are determined as shown in equation (A4). The same expression can also be obtained from equation (37) by simply replacing M_β with $M_{\Delta e}$, and I_β with $I_{\Delta e}$. Adding these additional terms to the right-hand side of equations (30) and (32) provides the complete set of inertia dynamic terms for these two hinge sequences.

$$\begin{aligned}
&-I_{\Delta e}\ddot{\beta} - \Omega^2\left(e_\beta M_{\Delta e}\sin\beta + \frac{1}{2} I_{\Delta e} \sin 2\beta\right) \\
&\quad - [(a_x \cos\psi - a_y \sin\psi)\sin\beta - a_z \cos\beta]M_{\Delta e} \\
&\quad + 2\Omega(p\cos\psi\cos\beta - q\sin\psi\cos\beta + r\sin\beta)(e_\beta M_{\Delta e} + I_{\Delta e}\cos\beta) \\
&\quad + [(\dot{q} + pr)\cos\psi\sin\beta + (\dot{p} - qr)\sin\psi\sin\beta \\
&\quad + (p^2 + q^2)\cos\beta](-M_{\Delta e}\ell_z + I_{\Delta e}\sin\beta) \\
&\quad + [(\dot{r} - pq)\cos\psi\sin\beta - (p^2 + r^2)\sin\psi\sin\beta + (\dot{p} + qr)\cos\beta] \\
&\quad \times [M_{\Delta e}(\ell_y + e_\beta \sin\psi) + I_{\Delta e}\sin\psi\cos\beta] \\
&\quad + [(q^2 + r^2)\cos\psi\sin\beta + (pq + \dot{r})\sin\psi\sin\beta - (\dot{q} - pr)\cos\beta] \\
&\quad \times [M_{\Delta e}(\ell_x - e_\beta \cos\psi) - I_{\Delta e}\cos\psi\cos\beta] \qquad \text{(A4)}
\end{aligned}$$

APPENDIX B

USEFUL TRANSFORMATION MATRICES

A list of useful transformation matrices is given in this appendix to facilitate the determination of the generalized forces in the Lagrange equations of motion, (25a) and (25b). Specific transformations of interest vary with the hinge sequences considered.

L-F-P Hinge Sequence

The frames of reference of particular interest for this hinge sequence are: x_1,y_1,z_1; x_3,y_3,z_3; and x,y,z. The components of an arbitrary vector a in these frames are related by

$$\begin{Bmatrix} a_{x_3} \\ a_{y_3} \\ a_{z_3} \end{Bmatrix} = \begin{bmatrix} \cos\zeta & -\sin\zeta & 0 \\ \sin\zeta & \cos\zeta & 0 \\ 0 & 0 & 1 \end{bmatrix} \begin{Bmatrix} a_{x_1} \\ a_{x_1} \\ a_{z_1} \end{Bmatrix} \tag{B1}$$

$$\begin{Bmatrix} a_x \\ a_y \\ a_z \end{Bmatrix} = \begin{bmatrix} \sin\psi & -\cos\psi & 0 \\ \cos\psi & \sin\psi & 0 \\ 0 & 0 & 1 \end{bmatrix} \begin{Bmatrix} a_{x_3} \\ a_{y_3} \\ a_{z_3} \end{Bmatrix} \tag{B2}$$

$$\begin{Bmatrix} a_{x_1} \\ a_{y_1} \\ a_{z_1} \end{Bmatrix} = \begin{bmatrix} \sin\psi\cos\zeta - \cos\psi\sin\zeta & \cos\psi\cos\zeta + \sin\psi\sin\zeta & 0 \\ -\sin\psi\sin\zeta - \cos\psi\cos\zeta & -\cos\psi\sin\zeta + \sin\psi\cos\zeta & 0 \\ 0 & 0 & 1 \end{bmatrix} \begin{Bmatrix} a_x \\ a_y \\ a_z \end{Bmatrix} \tag{B3}$$

Since these transformations are orthogonal, the inverse transformations are obtained by a simple transposition of the transformation matrices.

F-P-L Hinge Sequence

The frames of interest are: x_1,y_1,z_1; x_3,y_3,z_3; and x,y,z. However, these are defined differently from the L-F-P hinge sequence (fig. 6). The components of a vector a in these three frames are related by the following transformation.

$$\begin{Bmatrix} a_{x_3} \\ a_{y_3} \\ a_{z_3} \end{Bmatrix} = \begin{bmatrix} \cos\theta & 0 & \sin\theta \\ 0 & 1 & 0 \\ -\sin\theta & 0 & \cos\theta \end{bmatrix} \begin{Bmatrix} a_{x_1} \\ a_{y_1} \\ a_{z_1} \end{Bmatrix} \tag{B4}$$

$$\begin{Bmatrix} a_x \\ a_y \\ a_z \end{Bmatrix} = \begin{bmatrix} \sin\psi & -\cos\psi\cos\beta & -\cos\psi\sin\beta \\ \cos\psi & \sin\psi\cos\beta & \sin\psi\sin\beta \\ 0 & -\sin\beta & \cos\beta \end{bmatrix} \begin{Bmatrix} a_{x_3} \\ a_{y_3} \\ a_{z_3} \end{Bmatrix} \tag{B5}$$

$$\begin{Bmatrix} a_{x_1} \\ a_{y_1} \\ a_{z_1} \end{Bmatrix} = \begin{bmatrix} \sin\psi\cos\theta + \cos\psi\sin\beta\sin\theta & \cos\psi\cos\theta - \sin\psi\sin\beta\sin\theta & -\cos\beta\sin\theta \\ -\cos\psi\cos\beta & \sin\psi\cos\beta & -\sin\beta \\ \sin\psi\sin\theta - \cos\psi\sin\beta\cos\theta & \cos\psi\sin\theta + \sin\psi\sin\beta\cos\theta & \cos\beta\cos\theta \end{bmatrix} \begin{Bmatrix} a_x \\ a_y \\ a_z \end{Bmatrix} \tag{B6}$$

F-L-P Hinge Sequence

The frames of interest are the same as those for F-P-L hinge sequence. However, with the pitch bearing now outboard of the lag hinge, the transformations reduce to:

$$\begin{Bmatrix} a_{x_3} \\ a_{y_3} \\ a_{z_3} \end{Bmatrix} = \begin{Bmatrix} a_{x_1} \\ a_{y_1} \\ a_{z_1} \end{Bmatrix} \tag{B7}$$

$$\begin{Bmatrix} a_x \\ a_y \\ a_z \end{Bmatrix} = \begin{bmatrix} \sin\psi & -\cos\psi\cos\beta & -\cos\psi\sin\beta \\ \cos\psi & \sin\psi\cos\beta & \sin\psi\sin\beta \\ 0 & -\sin\beta & \cos\beta \end{bmatrix} \begin{Bmatrix} a_{x_3} \\ a_{y_3} \\ a_{z_3} \end{Bmatrix} \tag{B8}$$

$$\begin{Bmatrix} a_{x_1} \\ a_{y_1} \\ a_{z_1} \end{Bmatrix} = \begin{bmatrix} \sin\psi & \cos\psi & 0 \\ -\cos\psi\cos\beta & \sin\psi\cos\beta & -\sin\beta \\ -\cos\psi\sin\beta & \sin\psi\sin\beta & \cos\beta \end{bmatrix} \begin{Bmatrix} a_x \\ a_y \\ a_z \end{Bmatrix} \tag{B9}$$

APPENDIX C

GENERALIZED FORCES FOR L-F-P AND F-P-L HINGE SEQUENCES

A detailed derivation for the generalized forces in the coupled flap-lag equations of motion for the F-L-P hinge sequence has been given earlier in the report. This appendix provides a summary of the results for the other two hinge sequences, i.e., L-F-P and F-P-L, using the same procedure for the F-L-P case.

L-F-P Hinge Sequence

Similar to equations (40a) and (40b) for the case of F-L-P hinge sequence, the generalized forces Q_{ζ_1} and Q_{β_1} in equations (26) and (27) also consist of four contributing sources, i.e., gravity force, aerodynamic forces, and forces from lag dampers and hub springs. The last two sources are the same as equation (56) for the case of F-L-P. The first two sources differ markedly from equations (46), (47), (52), and (53) as shown below.

Gravity force contribution- The virtual displacement is developed from equation (2) to yield

$$\begin{aligned}
\delta x &= r_\beta \sin\beta \cos(\psi - \zeta)\delta\beta - (\Delta e + r_\beta \cos\beta)\sin(\psi - \zeta)\delta\zeta \\
\delta y &= -r_\beta \sin\beta \sin(\psi - \zeta)\delta\beta - (\Delta e + r_\beta \cos\beta)\cos(\psi - \zeta)\delta\zeta \\
\delta z &= -r_\beta \cos\beta\delta\beta
\end{aligned} \tag{C1}$$

for a blade element outboard of the flapping hinge, and

$$\begin{aligned}
\delta x &= -r_\zeta \sin(\psi - \zeta)\delta\zeta \\
\delta y &= -r_\zeta \cos(\psi - \zeta)\delta\zeta \\
\delta z &= 0
\end{aligned} \tag{C2}$$

for inboard of the flapping hinge. Substituting equations (41), (42), (C1), and (C2) into (39), the gravity force contribution to the generalized forces Q_{β_1} and Q_{ζ_1} is obtained.

$$Q_{\beta,G} = gM_\beta\{[A_1 \cos(\psi - \zeta) - A_2 \sin(\psi - \zeta)]\sin\beta - A_3 \cos\beta\} \tag{C3}$$

$$Q_{\zeta,G} = -g(\Delta em_\beta + M_\beta \cos\beta + M_{\Delta e})[A_1 \sin(\psi - \zeta) + A_2 \cos(\psi - \zeta)]$$

Contribution of the aerodynamic forces- With reference to figure C1, the elementary lift and drag, dL and dD, as given by equation C5),

$$\begin{aligned} dD &= (1/2)\rho U^2 c_d c\, dr_\beta \\ dL &= (1/2)\rho U^2 c_\ell c\, dr_\beta \\ U^2 &= u_T^2 + u_P^2 \\ \phi_r &= \tan^{-1}(u_P/u_T) \end{aligned} \tag{C5}$$

are first resolved in the plane perpendicular to the blade span,

$$\begin{aligned} dD_1 &= dD \cos \phi_r - dL \sin \phi_r \\ dL_1 &= dL \cos \phi_r + dD \sin \phi_r \end{aligned} \tag{C6}$$

and then in the x_1, y_1, z_1 frame of reference as shown in equation (C7)

$$\begin{Bmatrix} X_1 \\ Y_1 \\ Z_1 \end{Bmatrix}_A = \begin{Bmatrix} -dD_1 \\ -dL_1 \sin \beta \\ -dL_1 \cos \beta \end{Bmatrix} \tag{C7}$$

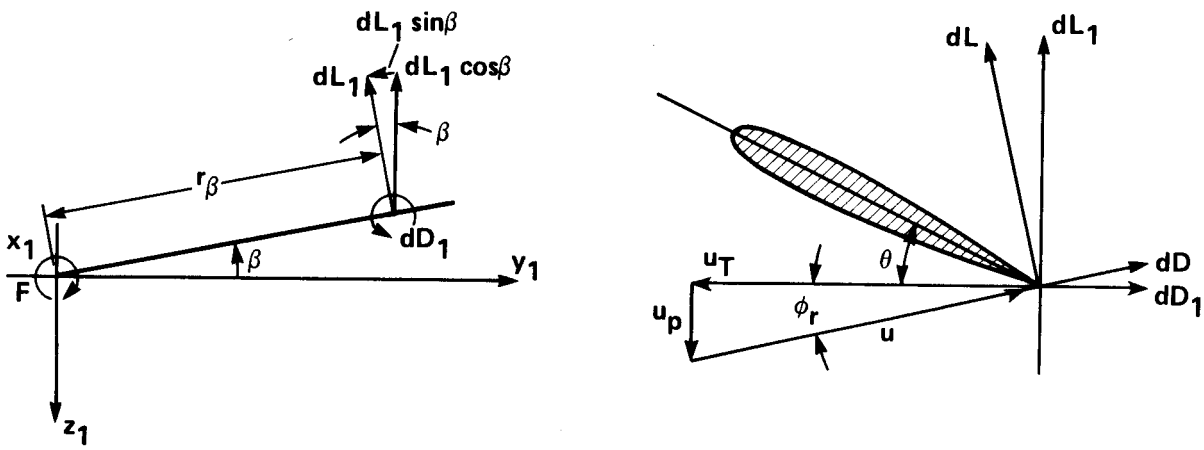

Figure C1.- Elemental lift and drag forces.

These aerodynamic force components are further resolved into the hub-body system to yield

$$\begin{Bmatrix} X_A \\ Y_A \\ Z_A \end{Bmatrix} = \begin{Bmatrix} -dD_1 \sin(\psi - \zeta) + dL_1 \cos(\psi - \zeta)\sin\beta \\ -dD_1 \cos(\psi - \zeta) - dL_1 \sin(\psi - \zeta)\sin\beta \\ -dL_1 \cos\beta \end{Bmatrix} \tag{C8}$$

Using equations (C8), (C1), (39b), and (39c), the aerodynamic force contributions to the generalized forces Q_{β_1} and Q_{ζ_1} are obtained.

$$Q_{\beta,A} = \int_{r_c}^{R} \frac{1}{2} \rho U^2 c_d c \sin\phi_r \, r_\beta \, dr_\beta + \int_{r_c}^{BR} \frac{1}{2} \rho U^2 c_\ell c \cos\phi_r r_\beta \, dr_\beta \tag{C9}$$

$$Q_{\zeta,A} = \int_{r_c}^{R} \frac{1}{2} \rho U^2 c_d c \cos\phi_r (\Delta e + r_\beta \cos\beta) dr_\beta - \int_{r_c}^{BR} \frac{1}{2} \rho U^2 c_\ell c \sin\phi_r (\Delta e + r_\beta \cos\beta) dr_\beta \tag{C10}$$

We note in passing that the transformation of the local airspeed at the blade element to u_T, u_S, and u_P, shown previously in equation (54) for the F-L-P case is now replaced by

$$\begin{Bmatrix} u_T \\ u_S \\ u_P \end{Bmatrix} = \begin{bmatrix} 1 & 0 & 0 \\ 0 & \cos\beta & -\sin\beta \\ 0 & \sin\beta & \cos\beta \end{bmatrix} \begin{Bmatrix} \dot{x}_1 \\ \dot{y}_1 \\ \dot{z}_1 \end{Bmatrix} \tag{C11}$$

The computation for the local angle of attack remains the same as that for the F-L-P hinge sequence using equations (55) and (49d).

F-P-L Hinge Sequence

The contributions due to the lag dampers and the hub springs are the same as equation (56), but the other two factors become somewhat more complicated than equations (46), (47), (52), and (53) as shown below.

Gravity force contribution- The virtual displacement is obtained from equation (14) for both outboard and inboard segments of the lag hinge. Proceeding in the same manner as before for the F-L-P hinge sequence results in equations (C12) and (C13).

$$Q_{\beta,G} = g[(\Delta e m_\zeta + M_\zeta \cos\zeta + M_{\Delta e})\sin\beta - M_\zeta \sin\zeta \cos\beta \sin\theta]$$
$$\times (A_1 \cos\psi - A_2 \sin\psi)$$
$$-g[(\Delta e m_\zeta + M_\zeta \cos\zeta + M_{\Delta e})\cos\beta + M_\zeta \sin\zeta \sin\beta \sin\theta]A_3 \qquad (C12)$$

$$Q_{\zeta,G} = gM_\zeta\{(\cos\beta \sin\zeta - \sin\beta \cos\zeta \sin\theta)(A_1 \cos\psi - A_2 \sin\psi)$$
$$- \cos\theta \cos\zeta(A_1 \sin\psi + A_2 \cos\psi) + (\sin\beta \sin\zeta + \cos\beta \cos\zeta \sin\theta)A_3\} \qquad (C13)$$

Aerodynamic force contributions- Using the same procedure as before for the F-L-P case, the aerodynamic force contributions to Q_{β_2} and Q_{ζ_2} are found to be

$$Q_{\beta,A} = \int_{r_c}^{BR} \frac{1}{2}\rho U^2 c_\ell c[\cos\phi_r \cos\theta(\Delta e + r_\zeta \cos\zeta)$$
$$+ \sin\phi_r \sin\theta(r_\zeta + \Delta e \cos\zeta)]dr_\zeta$$
$$- \int_{r_c}^{R} \frac{1}{2}\rho U^2 c_d c[\cos\phi_r \sin\theta(r_\zeta + \Delta e \cos\zeta)$$
$$- \sin\phi_r \cos\theta(\Delta e + r_\zeta \cos\zeta)]dr_\zeta \qquad (C14)$$

$$Q_{\zeta,A} = \int_{r_c}^{R} \frac{1}{2}\rho U^2 c_d c \cos\phi_r r_\zeta \, dr_\zeta - \int_{r_c}^{BR} \frac{1}{2}\rho U^2 c_\ell c \sin\phi_r r_\zeta \, dr_\zeta \qquad (C15)$$

The transformation (54) remains valid for computing the u_P, u_T, and u_S from the local airspeed at the blade element in x_1,y_1,z_1 frame of reference. Equation (B6) in turn provides the necessary transformation of the local airspeed components from the hub-body system to x_1,y_1,z_1 system.

The computation of the local angle of attack requires a special treatment for the F-P-L hinge sequence, because in this case ϕ_r specifically contains the blade pitch θ and its time derivative $\dot{\theta}$, as evident from equations (16) and (17). It should be noted also that the inertia dynamics for this hinge sequence require

values of θ and $\dot{\theta}$ as input quantities. Let θ_{vpo} be the root collective pitch when the lag hinge is parallel to the z axis. Then θ is given by (ref. 10)

$$\theta = \theta_o - \theta_{vpo} - A_{1s} \cos \psi - B_{1s} \sin \psi - K_1\beta - K_2\zeta \tag{C16}$$

Thus, in general,

$$\dot{\theta} = \dot{\theta}_o - (\dot{A}_{1s} + B_{1s}\Omega)\cos \psi - (\dot{B}_{1s} - A_{1s}\Omega)\sin \psi - K_1\dot{\beta} - K_2\dot{\zeta} \tag{C17}$$

Finally, the local angle of attack is:

$$\alpha_r = \phi_r + \theta_{vpo} + \theta_{t,r} \tag{C18}$$

REFERENCES

1. Schindler, R.; and Pfisterer, E.: Impacts of Rotor Hub Design Criteria on the Operational Capabilities of Rotorcraft Systems. Paper presented at AGARD Symposium on Rotorcraft Design for Operations, Amsterdam, The Netherlands, Oct. 1986.

2. Reichert, G.: Basic Dynamics of Rotors Control and Stability of Rotary Wing Aircraft, Aerodynamics and Dynamics of Advanced Rotary-Wing Configurations. AGARD-LS-63, Mar. 1973, pp. 3-1 to 3-50.

3. Howlett, J. J.: UH-60A Black Hawk Engineering Simulation Program: Vol. I - Mathematical Model. NASA CR-66309, 1981.

4. Morduchow, M.; and Hinchey, F. G.: Theoretical Analysis of Oscillations in Hovering of Helicopter Blades with Inclined and Offset Flapping and Lagging Hinge Axes. NASA TN 2226, 1950.

5. Jenkins, J. L., Jr.: A Numerical Method for Studying the Transient Blade Motions of a Rotor with Flapping and Lead-Lag Degrees of Freedom. NASA TND 4195, 1967.

6. Bramwell, A. R. S.: Helicopter Dynamics. John Wiley & Sons, 1976.

7. Johnson, W.: Helicopter Theory. Princeton Univ. Press, 1980.

8. Peters, D. A.; and Ormiston, R. A.: The Effects of Second-Order Blade Bending on the Angle of Attack of Hingeless Rotor Blades. J. AHS, vol. 18, no. 4, Oct. 1973, pp. 45-48.

9. Kaza, K. R. V.; and Kvaternik, R. G.: Examination of the Flap-Lag Stability of Rigid Articulated Rotor Blades. J. Aircraft, vol. 16, no. 12, Dec. 1979, pp. 876-884.

10. Chen, R. T. N.; and Davis, J. M.: Coupled Flap-Lag Rotor Analysis. Boeing Vertol Aero. Inv. III-272, Aug. 3, 1965.

11. Du Val, R. W.: Inertial Dynamics of a General Purpose Rotor Model. NASA TM-78557, 1979.

12. Blake, B. B.; Albion, N.; and Radford, R.: Flight Simulation of the CH-46 Helicopter. Paper presented at the 25th AHS National Forum, May 1969.

13. Wilcook, T.: RAE Experience in the Use of a Piloted Ground-Based Simulator for Helicopter Handling Studies. AGARD CP-121, Feb. 1973.

14. Chen, R. T. N.: Effects of Primary Rotor Parameters on Flapping Dynamics. NASA TP-1431, 1980.

15. Talbot, P. D.; Tinling, B. E.; Decker, W. A.; and Chen, R. T. N.: A Mathematical Model of a Single Main Rotor Helicopter for Piloted Simulation. NASA TM-84281, Sept. 1982.

16. Harendra, P. B.; Joglekar, M. J.; Gaffey, T. M.; and Marr, R. L.: V/STOL Tilt Rotor Study - Vol. V. A Mathematical Model for Real-Time Flight Simulation of the Bell Model 301 Tilt Rotor Research Aircraft. NASA CR-114614, 1973.

17. Hall, W. E., Jr.; and Bryson, A. E., Jr.: Inclusion of Rotor Dynamics in Controller Design. J. Aircraft, vol. 10, Apr. 1973, pp. 100-206.

18. Chen, R. T. N.; and Hindson, W. S.: Influence of High-Order Dynamics on Helicopter Flight Control System Bandwidth. J. Guidance, Control, and Dynamics, vol. 9, no. 2, 1986, pp. 190-197.

19. Hilbert, K. B.; Lebacqz, J. V.; and Hindson, W. S.: Flight Investigation of a Multivariable Model-Following Control System for Rotorcraft. AIAA Paper 86-9779, Apr. 1986.

20. Curtiss, H. C., Jr.: Stability and Control Modelling. Twelfth European Rotorcraft Forum, Garmisch-Patenkirchen, FRG, Sept. 1986.

21. Miller, D. G.; and White, F.: A Treatment of the Impact of Rotor-Fuselage Coupling on Helicopter Handling Qualities. Presented at the AHS Annual National Forum, St. Louis, MO, May 1987.

22. Goldstein, H.: Classical Mechanics. Addison-Wesley, 1950.

23. Wells, D. A.: Lagrangian Dynamics. McGraw-Hill Co., 1967.

24. Prouty, R. W.: A State-of-the-Art Survey of Two-Dimensional Airfoil Data. J. AHS, vol. 20, no. 4, Oct. 1975, pp. 14-25.

25. Harris, F. D.: Preliminary Study of Radial Flow Effects on Rotor Blades. J. AHS, vol. 11, no. 3, July 1966, pp. 1-21.

26. Harris, F. D.; Tarzanin, F. J., Jr.; and Fisher, R. K., Jr.: Rotor High Speed Performance, Theory vs. Test. J. AHS, vol. 15, no. 3, July 1970, pp. 35-44.

27. Ericsson, L. E.; and Reding, J. P.: Dynamic Stall of Helicopter Blades. J. AHS, vol. 17, no. 1, Jan. 1972, pp. 11-19.

28. McCroskey, W. J.; McAlister, K. W.; Carr, L. W.; Pucci, S. L.; Lambert, O.; and Lt. Indergrand, R. F.: Dynamic Stall on Advanced Airfoil Sections. J. AHS, vol. 26, no. 3, July 1981, pp. 40-50.

29. Leiss, U.: Semi-Empirical Simulation of Steady and Unsteady Rotor Blade Aerodynamic Loading. Paper presented at the 1st International Conf. on Rotorcraft Basic Research, Research Triangle Park, NC, Feb. 1985.

30. Pitt, D. M.; and Peters, D. A.: Theoretical Prediction of Dynamic-Inflow Derivatives. Vertica 5, 1981, pp. 21-34.

NASA National Aeronautics and Space Administration

Report Documentation Page

1. Report No.	2. Government Accession No.	3. Recipient's Catalog No.
NASA TM-100023		

4. Title and Subtitle

Flap-Lag Equations of Motion of Rigid, Articulated Rotor Blades with Three Hinge Sequences

5. Report Date

November 1987

6. Performing Organization Code

7. Author(s)

Robert T. N. Chen

8. Performing Organization Report No.

A-87338

10. Work Unit No.

505-61-51

9. Performing Organization Name and Address

Ames Research Center
Moffett Field, CA 94035-5000

11. Contract or Grant No.

13. Type of Report and Period Covered

Technical Memorandum

12. Sponsoring Agency Name and Address

National Aeronautics and Space Administration
Washington, DC 20546-0001

14. Sponsoring Agency Code

15. Supplementary Notes

Point of Contact: Robert T. N. Chen, Ames Research Center, M/S 211-2
Moffett Field, CA 94035-5000 (415) 694-5008 or
FTS 464-5008

16. Abstract

This report documents a derivation of coupled flap-lag equations of motion for a rigid articulated rotor with hinge springs and viscous dampers. Three different flapping-lag-pitch hinge sequences are considered and the Lagrange method is used in deriving the equations. The effects of the complete six degrees-of-freedom aircraft motions are included and all the inertia dynamic terms are retained; no small-angle assumptions are used in the development. Comparisons of the results of this work with those available in the literature are made. Sources of terms missing in previous analyses, especially those of the inertia dynamics, are identified.

17. Key Words (Suggested by Author(s))	18. Distribution Statement
Flapping, Lead-lag, Feathering, Equation of motion, Inertia dynamics Aerodynamic forces, Hinge sequences Lagrangian	Unclassified-Unlimited Subject Category - 08

19. Security Classif. (of this report)	20. Security Classif. (of this page)	21. No. of pages	22. Price
Unclassified	Unclassified	61	A04

NASA FORM 1626 OCT 86

For sale by the National Technical Information Service, Springfield, Virginia 22161